Supporting Information

Molecular Engineering of AIE-Active Boron Clustoluminogens for Enhanced Boron Neutron Capture Therapy

General information

1. Chemicals and materials

Unless otherwise stated, all the reactions were carried out under argon atmosphere with standard Schlenk techniques and all organic solvents were freshly distilled. All the available reagents were purchased from commercial sources and used directly. All the carborane-substituted compounds were synthesized from the corresponding alkynyl compounds according to the references. Reactions were monitored with thin layer chromatography (TLC) and column chromatography was operated on silica gel 200-300 mesh (Qingdaohaiyang Chem. Co).

The ^{1}H, ^{13}C and ^{11}B NMR spectra were measured at 298 K by using Bruker DRX-500 or Bruker 400. $CDCl_3$ and DMSO were used as the deuterated reagent unless specified. Mass spectra were conducted at Micromass Q-Tof instrument (ESI) and Agilent Technologies 5973N (EI). IR spectra were recorded on FT-IR spectrometer. Fluorescence spectra measurements were carried out by using a three-dimensional fluorescence spectrometer (HORIBA Nanolog, USA). Electronic absorption spectra were recorded with Shimadzu UV-2550 spectrophotometer.

2. Stability, photophysical property studies

The stability of all the compounds in the solution was investigated by monitoring the UV-vis spectra the target compounds in 20 μM solution (PBS buffer solution, pH = 7.4) over 72 h at 298 K. The results were shown in Figure S10. The absorption peaks of all the compounds had no observable change with time, indicating that the compounds are stable.

The fluorescence of the compounds was also conducted by a fluorescence spectrophotometer. The five compounds show very good fluorescence intensity in vitro and the structures are stable. The stability and fluorescence properties of the compounds provide the basis for subsequent cell experiments.

The absolute quantum yields of aggregated **NapE** compounds in toluene were detected by a three-dimensional fluorescence spectrometer (HORIBA Nanolog, USA). The absolute quantum yield is defined as the ratio of the number of photons emitted from a sample to that absorbed by the sample. For **NapE** compounds (10 μM) in toluene solution, the excitation wavelength is 365 nm, while pure toluene was set as the control. Then, the absolute quantum yields were calculated by the Measurement Software U6039-05.

Photon correlation spectroscopy and microelectrophoresis were used to determine the size and zeta potential, respectively, using a Malvern Z-sizer 5000 instrument. The morphological examination of compounds was performed with TEM (JEM-2100, JEOL, Japan).

3. DFT calculations

The DFT calculations were performed with Gaussian 16[1] to investigate the geometrical and electronic properties of the investigated compounds at the molecular level.

4. Cell culture and animals

The human non-small cell lung cancer cells A549 and H2228 were purchased from the Cell Resource Center of the Shanghai Academy of Sciences, CAS and preserved by our laboratory. A549 and H2228 cells were cultured in F-12 Kaighn's Modification medium (F-12K) and Roswell Park Memorial Institute-1640 medium (RPMI-1640), respectively, which contain 10 % bovine calf serum (HyClone, Logan, UT), and incubated at 37 °C in a 5 % CO_2 atmosphere. Female Balb/C-nude mice (4 weeks old, 20 g in weight) were purchased from Cavens Laboratory Animal Co. LTD (China) and housed in sterile barrier conditions in 12 h light/12 h dark cycles according to the animal care facility at Nanjing First Hospital. All in vivo experiments were approved by the Animal Care and Use Committee and Ethics Committee of Nanjing First Hospital (DWSY-23058362). All animals were acclimatized to the environment for at least one week to reduce stress before all animal experiments.

5. Cell viability assay

The in vitro cell viability of compounds was assessed with the CCK8 proliferation assay following the protocol of the manufacturer. The adherent A549 cells as well as H2228 cells were seeded in wells of 96-well plate (1×10^3 cells per well) and were incubated with different concentrations of compounds for 24 h, 48 h and 72 h. Then, cells were washed with fresh medium and CCK8 reagent was added to each well. After incubation for 2 h at 37 ℃, the OD value was detected on an enzyme-labeled instrument at 450 nm wavelength.

6. Subcutaneous xenograft model of lung cancer

All animal experiments were conducted by the standards approved by the Nanjing First Hospital Ethics Committee. Approximately 1×10^6 A549 cells suspended in 100 μL of PBS were subcutaneously implanted into the right shoulder of Balb/C-nude mice. The mice were kept under specific pathogen-free conditions, handled, and maintained by the guidelines of the Institutional Animal Care and Use Committee. When the size of the xenograft reached approximately 4 mm in diameter, the next experiments were performed. Tumor volumes were estimated using the formula: 0.5 × length × width × width.[2]

7. Cell uptake studies

We determined the cellular boron contents by ICP-MS: A549 cells were cultured in 6-well plates and allowed to reach a density of 70 % – 80 % on the subsequent day. Then, the cells were incubated with culture medium containing 60 μM **NapE4-5** for 24 h, 48 h and 72 h, respectively. Subsequently, the cells were washed with PBS buffer solution for three times, harvested by trypsinization, washed with fresh culture medium and counted. Then, 3×10^5 cells were finally resuspended in 500 μL conc. nitric acid (ultratrace analysis grade, Nanjing Reagent, China) for digestion. Boron contents in 3×10^5 cells treated with different concentrations of compounds were measured by ICP-MS for three times. The ICP-MS measurement was performed as follows: The digested samples were diluted with deionized water to a final volume of 4 mL and transferred to a polypropylene tube. The samples were then introduced into the ICP-MS system (Agilent 7700x, Agilent Technologies, Inc, USA) through a peristaltic pump and a

nebulizer. The boron contents were determined by using ^{11}B as the analyte. The calibration curve was obtained by using standard solutions of boron with known contents.

8. Cellular internalization of compounds and immunofluence

Fifty percent of confluent cells were cultured on glass coverslips in the wells of 24-well plates for 24 h. Then, the cells were incubated with culture medium containing **NapE4-5** (60 μM) for 24 h, 48 h and 72 h, respectively. Subsequently, the cells were washed, fixed, and permeabilized with 0.5% Triton X-100 for 10 min. After blocking with goat serum for 1 h, cells were incubated for 12 h with anti-EGFR antibody (1 : 30 dilution) (Proteintech, Chicago, USA). Then, dishes were washed and incubated with Alexa Fluor 488 or Alexa Fluor 594-conjugated secondary antibodies (1 : 50 dilution) (Thermo Fisher Scientific, USA) for 1 h at room temperature. Nuclei were stained with Hoechst33342 (10 μg/mL) (Beyotime, China) for 2 min. Then samples were examined with a fluorescence microscope (Zeiss, Oberkochen, Germany).

9. Biodistribution studies

The distribution and clearance of compounds in vivo were evaluated by measuring the boron content in mouse tissues at different times after injection. A total dose of 15 mg/kg of compounds was injected into the A549 tumor-bearing Balb/c-nude mice by tail vein injection when the tumor volume reached 40 − 70 mm^3. Mice were euthanized and dissected at 2 h, 8 h, 12 h, 24 h, 48 h and 72 h after injection. At specific time points, the boron content in blood and organs was assessed: brain, lung, heart, liver, kidney, spleen, tumor, blood, stomach and intestine were weighed and subsequently digested with 1 mL conc. nitric acid (ultratrace analysis grade, Nanjing Reagent, China) at 90 °C for 1 – 3 h. The digested samples were diluted to 10 mL with deionized water and transferred to a polypropylene tube before analysis. After filtering through a hydrophobic filter, boron contents of different tissues were determined by ICP-MS (Agilent 7700x; Agilent Technologies, USA).

10. Histopathology examination

The effects of compounds on organ morphology were assessed by histological analysis. Compounds (15 mg/kg) were intravenously injected into A549 tumor-bearing Balb/c-nude mice (n = 3). One week later, the organs (heart, liver, spleen, kidney, lung and others) were dissected, cleaned and stained with hematoxylin and eosin (H&E). PBS-injected mice (n = 3) served as controls.

11. In vivo real-time imaging

Luminescence images of whole mice bodies and isolated organs were obtained using the Maestro EX fluorescence imaging system (Cambridge Research & Instrumentation, CRi, USA). After being injected with compounds (15 mg/kg), mice underwent the whole-body luminescence imaging and then were sacrificed to isolate organs for the luminescence imaging. The samples were excited at 455 nm for imaging of **NapE4-5** and the signals were received at 500 − 670 nm and 580 − 750 nm, respectively. Acquire spectral fluorescence images of the probes and analyze them using Maestro software based on their spectral patterns. The intensities of the probe signals were calculated with de-mixed images by the Maestro software. The images captured at different time points under the same conditions were collected and re-processed by the Maestro software to share the same scale bar (n = 6).

12. Neutron irradiation on cells

All cell irradiation experiments were carried out at Xiamen Humanity Hospital-Neuboron BNCT Center using the NeuPex^{TM} Block-I AB-BNCT system. The A549 cells were seeded in 6-well plates at a density of 5×10^5 cells per well and incubated for 24 h. Then they were exposed to different concentrations (0, 30, 45 and 60 μM) of **^{10}B-NapE4** for 48 h at 37 °C in a humidified incubator. After removal of the **^{10}B-NapE4**-containing medium, the cells were washed with PBS, detached with trypsin and washed again three times with PBS. They were transferred to expend tubes and irradiated for either 17 min (low dose) or 26 min (high dose) (epithermal neutron flux: 8.015×10^8 n cm $^{-2}$ s $^{-1}$). After irradiation, the cells were reseeded in 6-well plates at a density of 200 cells per well for colony formation assay and in 96-well plates at a density of 1×10^4 cells per well for CCK8 assay. The cells were incubated for 24 h, 48 h and 72 h and the cell viability was measured by CCK8 assay according to the instructions of the manufacturer at each time point.

13. Colony formation assay

The cells in 6-well plate were incubated in 5 % CO_2 at 37 ℃ for 14 days. Then they were fixed with methanol and stained with crystal violet (0.04 % in water). The clones were photographed and recorded.

14. Neutron irradiation on tumor-bearing mice

The A549 tumor-bearing mice received intravenous injections of 15 mg/kg of **^{10}B-NapE4** one day before neutron irradiation. Exposure different times of each group of mice to neutron beams on the NeuPex^{TM} Block-I AB-BNCT system (Epithermal neutron flux: 8.015×10^8 n cm^{-2} s^{-1}): L BNCT (**^{10}B-NapE4** + exposure time of 7 min (Radioactive dosage statistical analysis was performed using Monte Carlo by tumors: 1.0 Gy)); M BNCT (**^{10}B-NapE4** + exposure time of 10 min (Radioactive dosage statistical analysis was performed using Monte Carlo by tumors: 1.5 Gy)); H BNCT (**^{10}B-NapE4** + exposure time of 14 min (Radioactive dosage statistical analysis was performed using Monte Carlo by tumors: 2.0 Gy)). The tumor volume and body weight of the mice were measured daily for 10 days using a caliper and a scale. The equation volume = (length × width × width)/2 was used to calculate the tumor volume.[2] The data were plotted and analyzed to evaluate the therapeutic effects of different groups. The mice were euthanized when the tumor size reached 2800 mm^3 or the weight loss exceeded 20 % (n = 6).

15. Immunohistochemistry

On the 10th day after irradiation, one mouse from each group was euthanized and the major organs (heart, liver, spleen, lung, kidney and so on) were collected and embedded in paraffin. The organs were sliced into ≈ 5 μm sections and stained with H&E for histological examination by light microscopy. The tumor tissues were removed and fixed for H&E, Ki67 and γ-H2AX staining for pathological analysis. Six to eight sections per animal were randomly selected and quantified.

16. Statistical analysis

Data are presented as mean ± standard deviation (SD) unless otherwise stated. Statistical analyses were performed using Prism version 8.0 (GraphPad Software, Inc.) and Excel (Microsoft). Unpaired, 2-tailed Student's t-test was used to compare two groups of data. One-way analysis of variance (ANOVA) followed by a post hoc test (Tukey) was used to compare multiple groups of data. A P value of less than 0.05 was considered statistically significant.

Synthesis of NapE compounds

To synthesize the "three-in-one" boron carriers, we initially used $B_{10}H_{12}(CH_3CN)_2$ precursor to react with the naphthalimide-substituted alkynes to obtain carborane-congugated naphthalimide intermediates in moderate yields. Subsequently, the targeted products of the **NapE** series compounds were generated through either classic Sonogashira reaction or copper(I)-catalyzed azide-alkyne cycloaddition reaction in high yields. In addition, the control compounds **NapE1-2** were also synthesized for comparison.

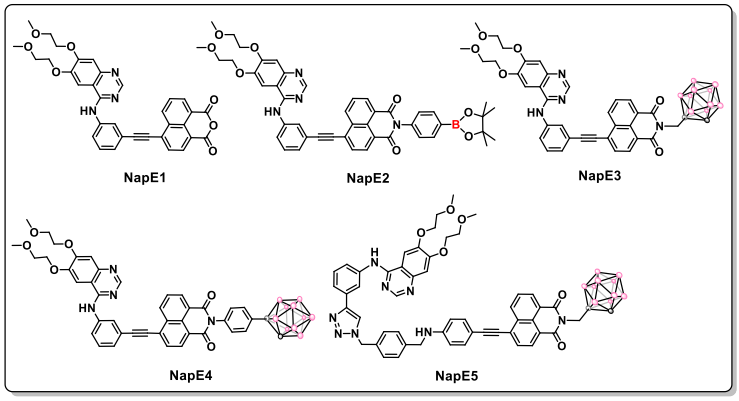

Figure S1. The new type of carborane-based boron carriers (five compounds).

1. The synthesis of NapE1

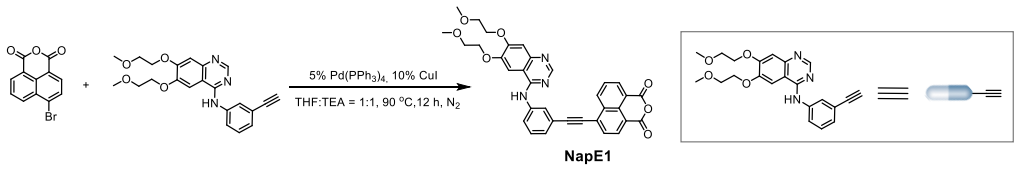

Scheme S1. Synthetic approach to **NapE1**.

NapE1： A mixture of 4-bromo-1,8-naphthalene dicarboxylic anhydride (1.00 equiv., 1mol) and Erlotinib (1.20 equiv., 1 mol), $Pd(PPh_3)_4$ (5.00 % mol), CuI (10.00 % mol) in mixed solvents (THF : TEA = 1:1) was refluxed for 24 h under argon. After cooling down to room temperature, the solvents were removed under vacuum and the residue was purified by column chromatography on silica gel. The crude mixture was separated on preparative TLC plates with solvents (volume ratio, DCM/MeOH: = 10 : 1) to afford the yellow solid. **Yield**: 87 %.

^{1}H NMR (400 MHz, $CDCl_3$) δ 8.83 (dd, *J* = 8.4, 1.0 Hz, 1H), 8.70 (s, 1H), 8.67 (dd, *J* = 7.3, 1.1 Hz, 1H), 8.59 (d, *J* = 7.6 Hz, 1H), 8.12 (s, 1H), 8.01 (d, *J* = 7.6 Hz, 1H), 7.90 (dd, *J* = 8.3, 7.4 Hz, 1H), 7.81 (dt, *J* = 7.6, 1.9 Hz, 1H), 7.51 – 7.42 (m, 3H), 7.28 (d, *J* = 7.4 Hz, 2H), 4.36 – 4.29 (m, 4H), 3.89 – 3.85 (m, 4H), 3.49 (d, *J* = 5.7 Hz, 6H).

^{13}C NMR (101 MHz, DMSO-*d*$_6$) δ 160.9, 160.7, 156.6, 154.1, 148.6, 140.4, 133.4, 133.3, 132.1, 131.7, 131.4, 130.2, 129.7, 129.1, 127.6, 127.3, 125.4, 124.2, 121.7, 120.2, 119.4, 103.6, 100.0, 86.1, 70.5, 68.8, 68.5, 58.8.

HRMS: *m/z* calcd for $C_{34}H_{27}N_3O_7[M+H]^+$: 590.1922. Found: 590.1920.

2. The synthesis of NapE2

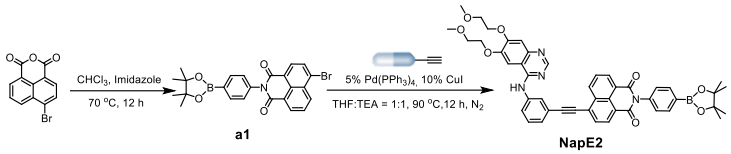

Scheme S2. Synthetic approach to **NapE2**.

a1: A mixture of 4-bromo-1,8-naphthalenedicarboxylic anhydride (1.38 g, 5.00 mmol), 4-(4,4,5,5-tetramethyl-1,3,2-dioxaborolan-2-yl)aniline (1.64 g, 7.50 mmol), and imidazole (6.80 g, 0.10 mol) in chloroform (40.0 mL) was stirred under reflux for 7 h and then cooled to room temperature. Subsequently, the solvent was removed by a rotary evaporator and the residue was taken up in a small amount of absolute ethanol. The resulting suspension was sonicated for 15 min, filtered, washed with cold ethanol and dried in air to afford **a1** as a white solid. **a1**, Yield: 90 %.

^{1}H NMR (400 MHz, $CDCl_3$) δ 8.71 (dd, J = 7.3, 1.0 Hz, 1H), 8.64 (dd, J = 8.5, 1.0 Hz, 1H), 8.46 (d, J = 7.9 Hz, 1H), 8.08 (d, J = 7.9 Hz, 1H), 8.00 (d, J = 8.3 Hz, 2H), 7.89 (dd, J = 8.5, 7.3 Hz, 1H), 7.32 (d, J = 8.3 Hz, 2H), 1.37 (s, 12H).

HRMS: *m/z* calcd for $C_{24}H_{21}BBrNO_4[M+H]^+$: 478.0820, Found: 478.0815.

NapE2 was synthesized according to **NapE1**. Yield: 78 %.

^{1}H NMR (400 MHz, DMSO-d_6) δ 9.55 (s, 1H), 8.82 (d, J = 8.4, 1H), 8.53 (s, 1H), 8.59 – 8.50 (m, 2H), 8.47 (d, J = 7.6 Hz, 1H), 8.24 (s, 1H), 8.13 (d, J = 7.6 Hz, 1H), 8.05 – 8.01 (m, 2H), 7.92 – 7.77 (m, 3H), 7.54 (d, J = 5.0 Hz, 2H), 7.43 (d, J = 8.2 Hz, 2H), 7.22 (s, 1H), 4.34 – 4.25 (m, 4H), 3.84 – 3.72 (m, 4H), 3.37 (d, J = 9.9 Hz, 6H), 1.34 (s, 12H).

^{13}C NMR (101 MHz, DMSO-d_6) δ 163.8, 163.5, 156.6, 154.1, 153.2, 148.6, 147.5, 140.5, 139.2, 135.3, 132.4, 131.7, 131.5, 131.4, 130.5, 129.6, 129.1, 128.7, 128.3, 127.1, 126.7, 125.2, 123.9, 123.6, 122.9, 121.8, 109.4, 108.6, 103.6, 99.3, 86.4, 84.3, 73.9, 70.6, 70.5, 68.8, 68.5, 58.9, 58.8, 49.0, 25.1.

HRMS: *m/z* calcd for $C_{46}H_{43}BN_4O_8[M+H]^+$: 791.3202, Found: 791.3207.

3. The synthesis of NapE3

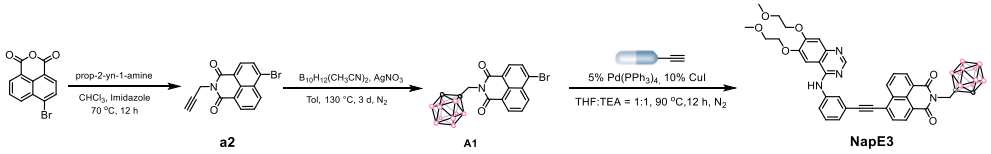

Scheme S3. Synthetic approaches to **NapE3**.

a2[3] was synthesized according to **a1**. Yield: 90 %.

^{1}H NMR (400 MHz, $CDCl_3$) δ 8.62 (d, J = 7.3 Hz, 1H), 8.52 (d, J = 9.1 Hz, 1H), 8.38 (d, J = 7.9 Hz, 1H), 7.98 (d, J = 7.9 Hz, 1H), 7.82 – 7.76 (m, 1H), 4.88 (d, J = 2.4 Hz, 2H), 2.14 (t, J = 2.4 Hz, 1H).

A1: A mixture of **a2** (1.0 equiv., 1 mol) and $B_{10}H_{12}(CH_3CN)_2$ (1.2 equiv., 1.2 mol), $AgNO_3$(10 % mol) in dry toluene was refluxed for three days under argon. After cooling down to room temperature, MeOH (50.0 mL) was then added to quench the reaction. Excessive solvents were removed under vacuum, then the crude product was purified by column chromatography using PE / DCM (v / v = 1 : 1) as eluent to afford **A1** as a white solid. Yield: 53 %.

^{1}H NMR (400 MHz, $CDCl_3$) δ 8.69 – 8.67 (m, 2H), 8.44 (d, J = 7.9 Hz, 1H), 8.10 (d, J = 7.9 Hz, 1H), 7.90 (dd, J = 8.4, 7.4 Hz, 1H), 4.92 (s, 2H), 4.19 (s, 1H, $H_{carborane}$), 2.82 – 1.75 (br, 10H, B−H).
^{13}C NMR (101 MHz, $CDCl_3$) δ 163.42, 163.32, 134.44, 133.09, 132.19, 131.68, 131.44, 130.86, 129.08, 128.37, 121.93, 121.00, 73.45, 61.13, 44.22.
^{11}B {^{1}H} NMR (128 MHz, $CDCl_3$) δ − 1.2 (1B), − 4.6 (1B), − 11.3 (8B).
HRMS: *m/z* calcd for $C_{15}H_{18}B_{10}BrNO_2[M+H]^+$: 432.1597, Found: 432.1545.

NapE3 was synthesized according to **NapE1**. Yield: 81 %.
^{1}H NMR (400 MHz, $CDCl_3$) δ 8.83 – 8.75 (m, 1H), 8.68 (s, 1H), 8.64 (d, J = 7.3 Hz, 1H), 8.58 – 8.52 (m, 1H), 8.12 (s, 1H), 7.97-7.94 (m, 1H), 7.90 – 7.84 (m, 1H), 7.78 – 7.79 (m, 1H), 7.61 (s, 1H), 7.45 – 7.42 (m, 2H), 7.27 (s, 1H), 7.24 – 7.23 (m, 1H), 4.92 (s, 2H), 4.30 – 4.27 (m, 4H), 4.21 (s, 1H, C−$H_{carborane}$), 3.87 – 3.80 (m, 4H), 3.48 (dd, J = 4.9, 2.0 Hz, 6H), 2.94 – 1.91 (br, 10H, B−H).
^{13}C NMR (101 MHz, $CDCl_3$) δ 163.7, 163.4, 156.2, 154.6, 153.5, 148.9, 147.6, 139.2, 133.5, 132.6, 131.7, 131.3, 130.9, 129.3, 128.7, 128.1, 127.7, 127.5, 124.6, 122.8, 122.6, 121.7, 120.7, 109.1, 108.8, 102.4, 99.8, 86.1, 73.5 ($C_{carborane}$), 70.9, 70.4, 69.2, 68.3, 61.1 ($C_{carborane}$), 59.3, 59.2, 44.2.
^{11}B {^{1}H} NMR (128 MHz, $CDCl_3$) δ − 1.3 (2B), − 10.0 (4B), − 12.6 (4B).
HRMS: *m/z* calcd for $C_{37}H_{40}B_{10}N_4O_6[M+H]^+$: 745.4024, Found: 745.4024.

4. The synthesis of NapE4

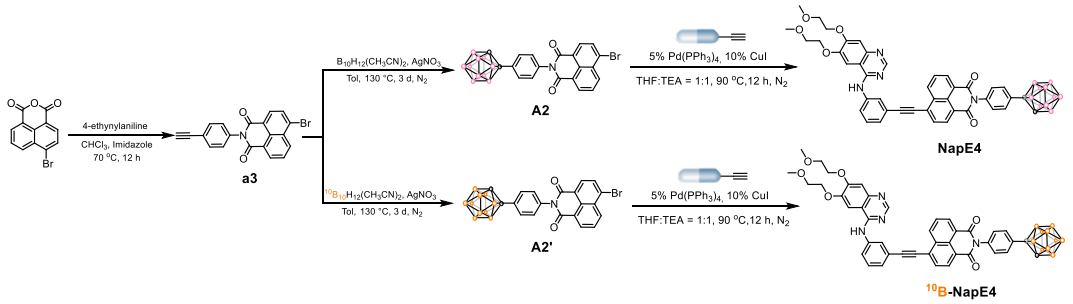

Scheme S4. Synthetic approaches to **NapE4** and **^{10}B-NapE4**.

a3 was synthesized according to **a1**. Yield: 92 %.
^{1}H NMR (400 MHz, $CDCl_3$) δ 8.71 (dd, J = 7.3, 1.0 Hz, 1H), 8.66 (dd, J = 8.5, 1.0 Hz, 1H), 8.47 (d, J = 7.9 Hz, 1H), 8.10 (d, J = 7.9 Hz, 1H), 7.90 (dd, J = 8.5, 7.4 Hz, 1H), 7.70 – 7.63 (m, 2H), 7.32 – 7.27 (m, 2H), 3.14 (s, 1H).
HRMS: *m/z* calcd for $C_{20}H_{10}BrNO_2[M+H]^+$: 375.9968, Found: 375.9968.

A2 was synthesized according to **A1**. Yield: 59 %.
^{1}H NMR (400 MHz, $CDCl_3$) δ 8.69-8.67 (m, 2H), 8.46 (d, J = 7.9 Hz, 1H), 8.10 (d, J = 7.9 Hz, 1H), 7.91 (dd, J = 8.5, 7.4 Hz, 1H), 7.68 (d, J = 8.7 Hz, 2H), 7.31 (d, J = 8.7 Hz, 2H), 4.01 (s, 1H, $H_{carborane}$), 2.92 – 1.73 (br, 10H, B−H).
^{13}C NMR (101 MHz, $CDCl_3$) δ 163.6, 163.5, 146.5, 136.7, 134.1, 133.7, 132.7, 131.8, 131.4, 131.2, 130.9, 129.4, 129.2, 128.9, 128.3, 122.9, 122.0, 75.8 ($C_{carborane}$), 60.42 ($C_{carborane}$).
^{11}B {^{1}H} NMR (128 MHz, $CDCl_3$) δ − 2.23 (2B), − 9.98 (8B).
HRMS: *m/z* calcd for $C_{23}H_{20}B10NO_2[M+H]^+$: 530.1753, Found: 530.1751.

NapE4 was synthesized according to **NapE1**. Yield: 87 %.

^{1}H NMR (400 MHz, $CDCl_3$) δ 8.82 (dd, *J* = 8.4, 0.9 Hz, 1H), 8.71 (s, 1H), 8.66 (dd, *J* = 7.3, 1.0 Hz, 1H), 8.61 (d, *J* = 7.7 Hz, 1H), 8.11 (s, 1H), 8.00 (d, *J* = 7.6 Hz, 1H), 7.92 – 7.87 (m, 1H), 7.82 (m, 1H), 7.68 – 7.64 (m, 2H), 7.48 (m, 2H), 7.31 (m, 4H), 7.24 (s, 1H), 4.34 – 4.29 (m, 4H), 3.99 (s, 1H, $H_{carborane}$), 3.90 – 3.83 (m, 4H), 3.50 (d, *J* = 5.1 Hz, 6H), 2.84 – 1.90 (br, 10H, B−H).

^{13}C NMR (101 MHz, DMSO-d_6) δ 163.2, 162.9, 156.5, 154.1, 151.5, 148.4, 145.1, 143.6, 139.1, 137.4, 133.6, 132.8, 132.2, 131.9, 131.2, 130.9, 129.9, 129.6, 129.1, 128.1, 127.9, 127.8, 127.6, 126.3, 125.5, 124.0, 122.9, 122.7, 122.2, 122.0, 121.4, 108.2, 105.8, 103.2, 98.8, 86.0, 76.4 ($C_{carborane}$), 70.0, 68.4, 68.2, 61.1 ($C_{carborane}$), 58.4.

^{11}B {^{1}H} NMR (128 MHz, $CDCl_3$) δ− 1.7 (2B), − 8.8 (2B), − 10.7 (6B).

HRMS: *m/z* calcd for $C_{42}H_{42}B_{10}N_4O_6[M+H]^+$: 807.4180, Found: 807.4167.

A2' was synthesized according to **A1**. Yield: 58 %.

^{1}H NMR (400 MHz, $CDCl_3$) δ 8.69-8.67 (m, 2H), 8.46 (d, *J* = 7.9 Hz, 1H), 8.10 (d, *J* = 7.9 Hz, 1H), 7.91 (dd, *J* = 8.5, 7.4 Hz, 1H), 7.68 (d, *J* = 8.7 Hz, 2H), 7.31 (d, *J* = 8.7 Hz, 2H), 4.00 (s, 1H, $H_{carborane}$), 2.98 – 1.94 (br, 10H, B−H).

^{13}C NMR (101 MHz, $CDCl_3$) δ 163.6, 163.5, 146.5, 136.7, 134.1, 133.7, 132.7, 131.8, 131.4, 131.2, 130.9, 129.4, 129.2, 128.9, 128.3, 122.9, 122.0, 75.8 ($C_{carborane}$), 60.42 ($C_{carborane}$).

HRMS: *m/z* calcd for $C_{23}H_{20}{}^{10}B10NO_2[M+H]^+$: 522.1753, Found: 522.1764.

^{10}B-NapE4 was synthesized according to **NapE4**, Yield: 46 %.

^{1}H NMR (400 MHz, DMSO-d_6) δ 9.60 (s, 1H), 8.87 (d, *J* = 8.4 Hz, 1H), 8.59 (d, *J* = 7.3 Hz, 1H), 8.54 – 8.49 (m, 1H), 8.26 (s, 1H), 8.17 (d, *J* = 7.7 Hz, 1H), 8.10 – 7.99 (m, 2H), 7.91 (s, 1H), 7.76 (d, *J* = 8.8 Hz, 2H), 7.67 – 7.53 (m, 4H), 7.50 (d, *J* = 8.7 Hz, 1H), 7.25 (s, 1H), 4.32 (m, 4H), 4.29 (s, 1H, $H_{carborane}$), 3.83 – 3.73 (m, 4H), 3.37 (d, *J* = 9.4 Hz, 6H), 2.76 – 1.89 (br, 10H, B−H).

^{13}C NMR (101 MHz, DMSO-d_6) δ 163.2, 163.0, 156.5, 154.0, 151.9, 148.3, 145.2, 143.9, 139.5,137.5, 133.7, 132.8, 132.0, 131.5, 131.3, 130.1, 129.7, 129.2, 128.8, 128.0, 127.8, 127.3, 126.7, 126.4, 125.8, 124.0, 123.2, 123.0, 122.5, 122.3, 121.4, 108.5, 106.6, 103.4, 98.8, 86.0, 76.5 ($C_{carborane}$), 70.0, 68.47, 68.2, 61.2 ($C_{carborane}$), 58.4.

HRMS: *m/z* calcd for $C_{42}H_{42}{}^{10}B_{10}N_4O_6[M+H]^+$: 799.4469, Found: 799.4463.

5. The synthesis of NapE5

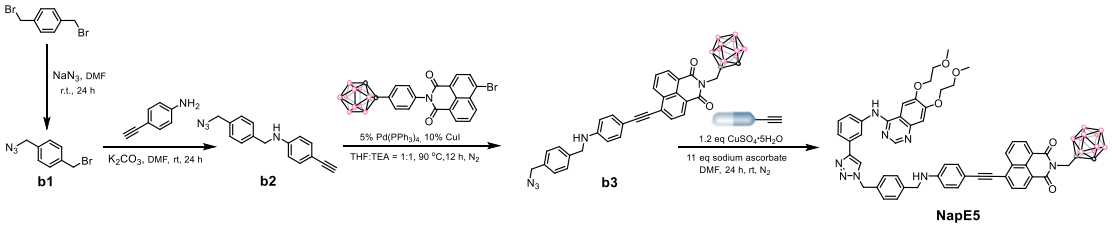

Scheme S5. Synthetic approaches to **NapE5**.

b1[4]: yield of 97 %.

^{1}H NMR (400 MHz, $CDCl_3$) δ 7.43 – 7.29 (m, 4H), 4.49 (d, *J* = 7.6 Hz, 2H), 4.35 (d, *J* = 6.2 Hz, 2H).

b2: yield of 85 %.

^{1}H NMR (400 MHz, $CDCl_3$) δ 7.81 (d, *J* = 8.8 Hz, 1H), 7.36 (d, *J* = 8.0 Hz, 2H), 7.29 (dd, *J* = 8.4, 4.5 Hz, 4H), 6.55 (m, *J* = 22.7, 8.8 Hz, 3H), 4.46 – 4.32 (m, 4H), 2.48 (s, 1H).

HRMS: *m/z* calcd for $C_{16}H_{14}N_4[M+H]^+$: 263.1291, Found: 263.1297.

b3 was synthesized according to **NapE1**. Yield: 88 %.
^{1}H NMR (400 MHz, $CDCl_3$) δ 8.75 (dd, *J* = 8.4, 1.1 Hz, 1H), 8.61 (dd, *J* = 7.3, 1.1 Hz, 1H), 8.49 (d, *J* = 7.7 Hz, 1H), 7.87 – 7.79 (m, 2H), 7.49 (d, *J* = 8.7 Hz, 2H), 7.39 (d, *J* = 8.1 Hz, 2H), 7.32 (d, *J* = 8.1 Hz, 2H), 6.65 (d, *J* = 8.7 Hz, 2H), 4.89 (s, 2H), 4.50 (m, 1H), 4.43 (d, *J* = 5.1 Hz, 2H), 4.35 (s, 2H), 4.20 (s, 1H, $H_{carborane}$), 3.02 – 1.70 (br, 10H, B−H).
^{13}C NMR (101 MHz, $CDCl_3$) δ 163.9, 163.6, 149.1, 138.7, 134.8, 133.9, 133.7, 132.5, 131.6, 131.5, 130.0, 128.7, 128.3, 127.8, 127.3, 121.7, 119.6, 112.7, 110.0, 102.5, 85.1, 73.7, 61.1, 54.5, 47.5, 44.2.
^{11}B {^{1}H} NMR (128 MHz, $CDCl_3$) δ − 1.87 (1B), − 4.11 (1B), − 10.36 (4B), − 12.20 (4B).
HRMS: *m/z* calcd for $C_{31}H_{31}B_{10}N_5O_2[M+H]^+$: 614.3554, Found: 614.3515.

NapE5: Erlotinib (1.00 equiv., 1 mol), **b3** (1.20 equiv., 1.2 mol), $CuSO_4 \cdot 5H_2O$ (1.20 equiv.) and sodium ascorbate (11.00 equiv.) were dispersed in DMF (20.0 mL). The resulting mixture was flushed with nitrogen and stirred at room temperature for 24 hours. The mixture was poured into water to furnish a precipitate. The precipitate was filtered and washed with water, then dried in an oven. The crude product was purified by column chromatography over DCM/MeOH = 10 : 1 (v / v) to yield the product of **NapE5**. Yield: 87 %.
^{1}H NMR (400 MHz, DMSO-d_6) δ 8.76 (d, *J* = 8.2 Hz, 1H), 8.61 (d, *J* = 6.4 Hz, 2H), 8.50 (d, *J* = 7.7 Hz, 1H), 8.11 (s, 1H), 7.91 – 7.74 (m, 4H), 7.70 (m, 2H), 7.50 – 7.44 (m, 3H), 7.38 (m, 3H), 7.29 (m, 2H), 7.19 (s, 1H), 6.62 (d, *J* = 8.6 Hz, 2H), 5.55 (s, 2H), 4.91 (s, 2H), 4.59 (s, 1H), 4.40 (d, *J* = 4.1 Hz, 2H), 4.27 – 4.23 (m, 4H), 4.21 (s, 1H, $H_{carborane}$), 3.85 – 3.79 (m, 4H), 3.45 (s, 6H), 2.84 – 1.95 (br, 10H, B−H).
^{13}C NMR (101 MHz, $CDCl_3$) δ 163.8, 163.5, 162.5, 156.3, 154.4, 153.5, 149.0, 148.9, 147.9, 147.3, 139.4, 139.3, 133.9, 133.6, 132.4, 131.5, 131.4, 131.1, 130.4, 130.0, 129.5, 128.4, 128.3, 128.2, 128.0, 127.3, 121.6, 121.4, 121.1, 119.9, 119.6, 118.6, 112.6, 110.0, 109.2, 108.7, 102.4, 102.3, 85.0, 73.7 ($C_{carborane}$), 70.8, 70.4, 69.1, 68.3, 61.1 ($C_{carborane}$), 59.3, 59.2, 53.9, 47.2, 44.1.
^{11}B {^{1}H} NMR (128 MHz, DMSO-d_6) δ − 1.3 (2B), − 10.1 (4B), − 12.6 (4B).
HRMS: *m/z* calcd for $C_{53}H_{54}B_{10}N_8O_6[M+H]^+$: 1007.5248, Found: 1007.5242.

Table S1. FTIR spectra, normalized UV-vis absorption spectra, and normalized PL spectra peaks of the compounds in mixed solvents (PBS buffer solution : DMSO = 95 : 5) at room temperature.

Compound	IR (B–H, cm^{-1})	λ_{abs} (nm)	λ_{em} (nm)
NapE1	--	348, 383	523
NapE2	--	347, 375	562
NapE3	2567	348, 383	568
NapE4	2577	346, 377	576
NapE5	2573	348, 455	664
^{10}B-NapE4	2574	347, 379	575

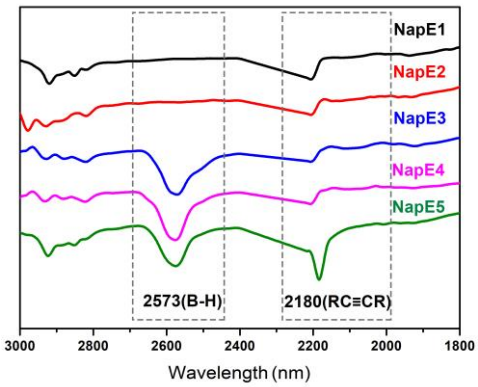

Figure S2. Fourier transform infrared spectra of **NapE1-5**.

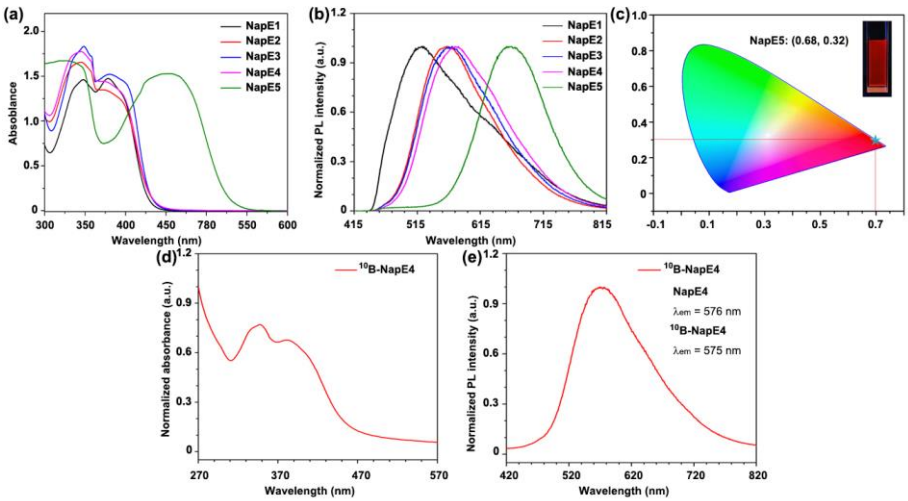

Figure S3. Normalized UV-vis absorption spectra (a) and normalized PL spectra (b) at room temperature (λ_{ex} = 365 nm) for **NapE1-5**; (c) CIE chromaticity coordinates of the **NapE5** (inset: luminescence photographs). (d) Normalized UV-vis absorption spectrum of **^{10}B-NapE4** at room temperature. (e) Normalized PL spectrum of **^{10}B-NapE4** at room temperature. All measurements in PBS buffer solution : DMSO = 95 : 5, c = 1.0×10 $^{-5}$ M.

Table S2. The fluorescence quantum yield and fluorescence lifetime of the compounds in toluene at room temperature.

Compounds	Φ (%)	τ (ns)
NapE1	46.87	2.37
NapE2	27.44	2.32
NapE3	27.21	2.00
NapE4	33.99	2.12
NapE5	73.03	1.32

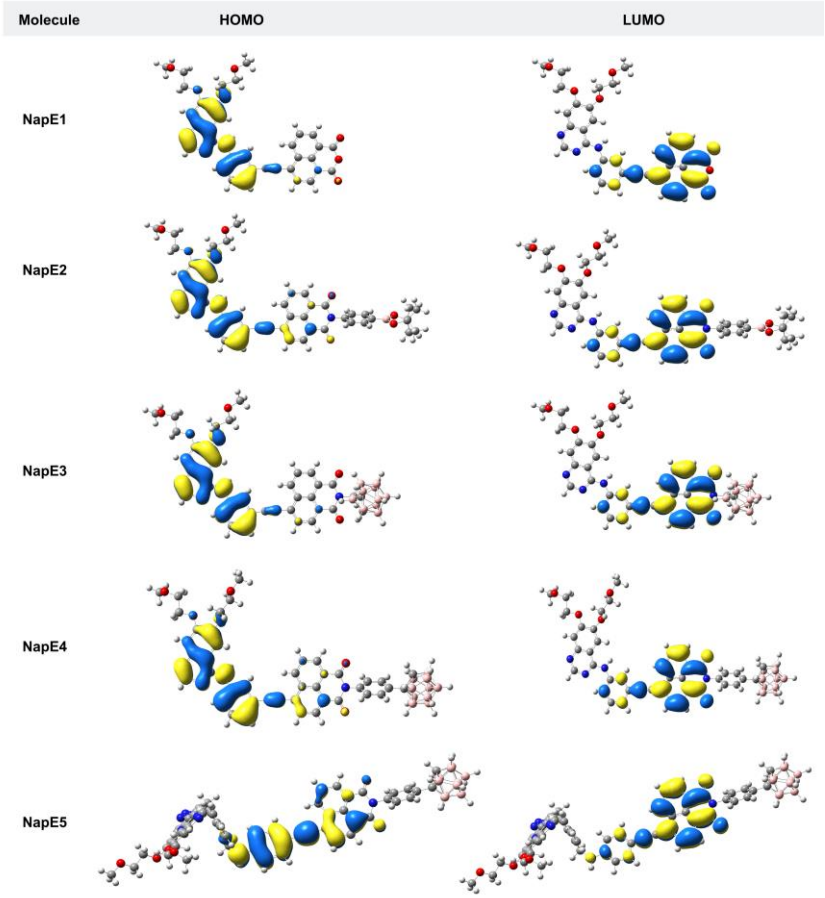

Figure S4. HOMO and LUMO distributions of **NapE1-5** calculated in the ground state.

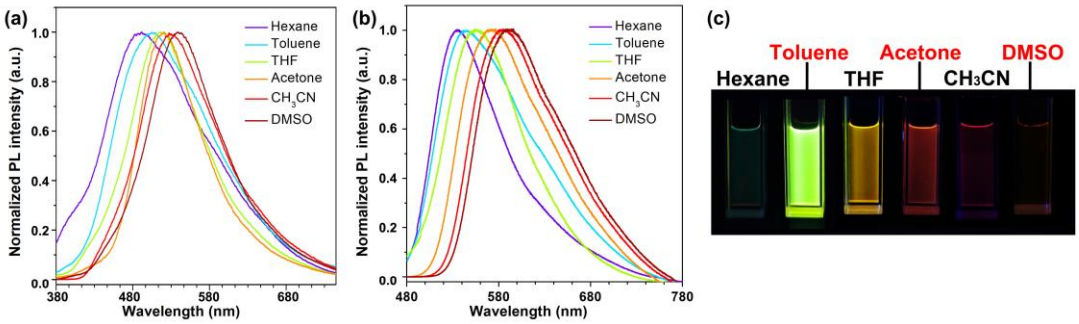

Figure S5. Normalized PL spectra of **NapE4** (a) and **NapE5** (b) (10 μM) in different solvents (λ_{ex} = 365 nm). (c) Luminescence photographs of **NapE5** (20 μM) in different solvents.

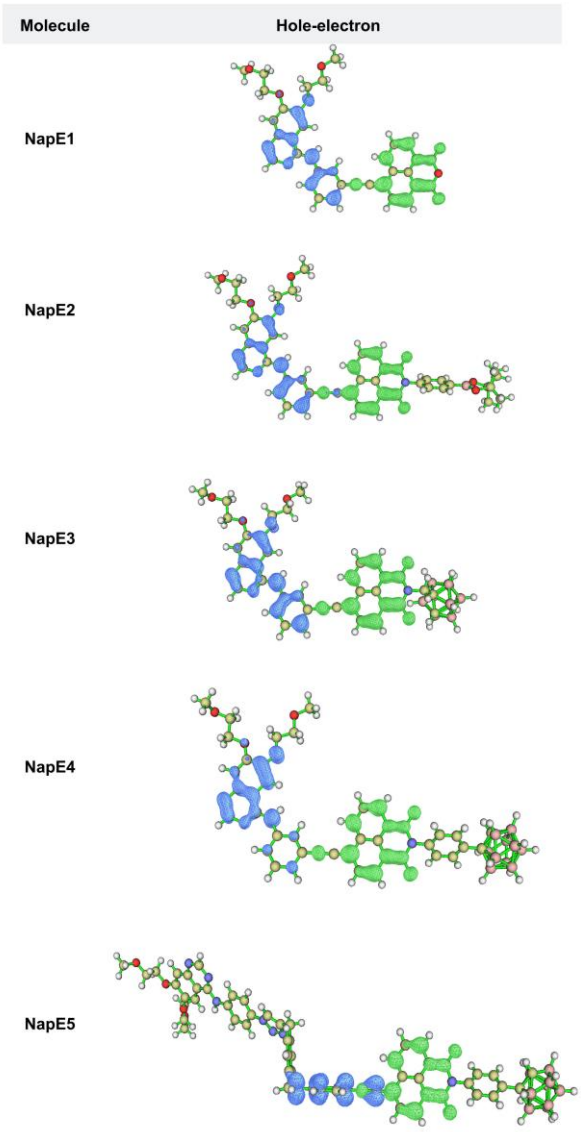

Figure S6. The electron and hole localization of the excited state (S_1) of **NapE1-5**.

Table S3. PL spectral peak values of **NapE1-5** (10 μM) in different solvents (λ_{ex} = 365 nm).

	λ_{em} (nm)					
Compounds	Hexane	Toluene	THF	Acetone	CH_3CN	DMSO
NapE1	480.7	495.5	499.7	501.9	505.8	510.5
NapE2	487.3	505.1	516.3	520.5	531.8	537.4
NapE3	483.1	493.3	504.3	518.8	528.1	541.3
NapE4	486.5	492.9	502.4	513.4	532.5	549.4
NapE5	533.9	544.3	555.8	570.1	582.4	595.4

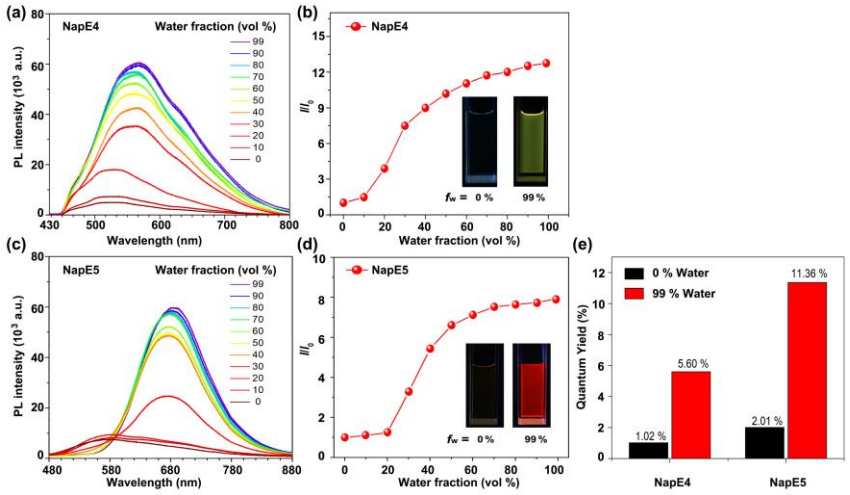

Figure S7. PL spectra of **NapE4** (a) and **NapE5** (c) in DMSO / water mixtures with different water fractions (f_w). The plot of the relative emission intensity (I/I_0) versus water fraction. I_0 and I are the peak values of PL intensities of **NapE4** (b) and **NapE5** (d) DMSO/water mixtures. Inset: luminescence photograph. (e) Absolute PL quantum yields of **NapE4-5** in solution and aggregated states (99 % fraction of water).

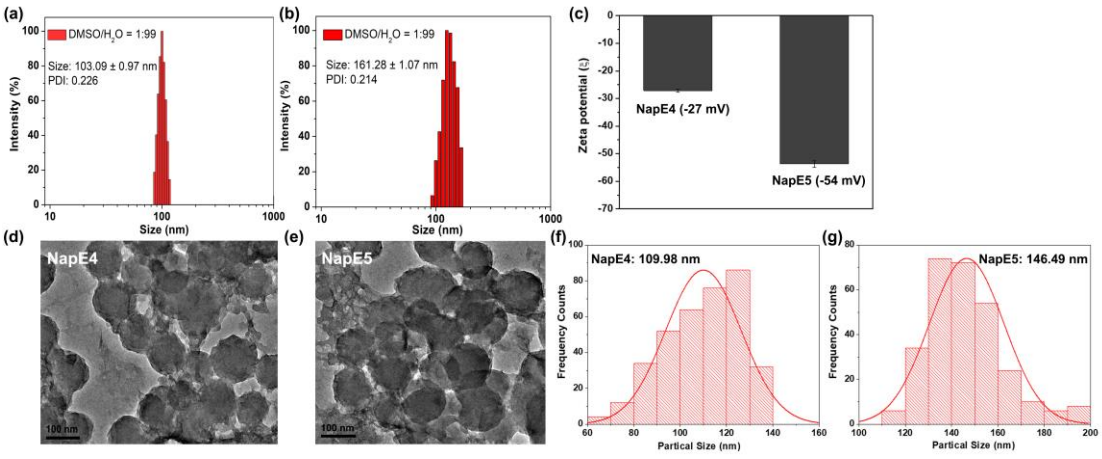

Figure S8. Size distribution of **NapE4** (a) and **NapE5** (b) from DLS experiments; (c) Zeta potentials of **NapE4** and **NapE5**; TEM images of **NapE4** (d) and **NapE5** (e) show spherical and uniform particles with an average size of 109.98 nm for **NapE4** and 146.49 nm for **NapE5**; The quantitative statistical histogram of particle size and distribution in the electron microscopy images of **NapE4** (f) and **NapE5** (g). Particles obtained from the mixed solvents of DMSO / H_2O (volume ratio: 1 / 99).

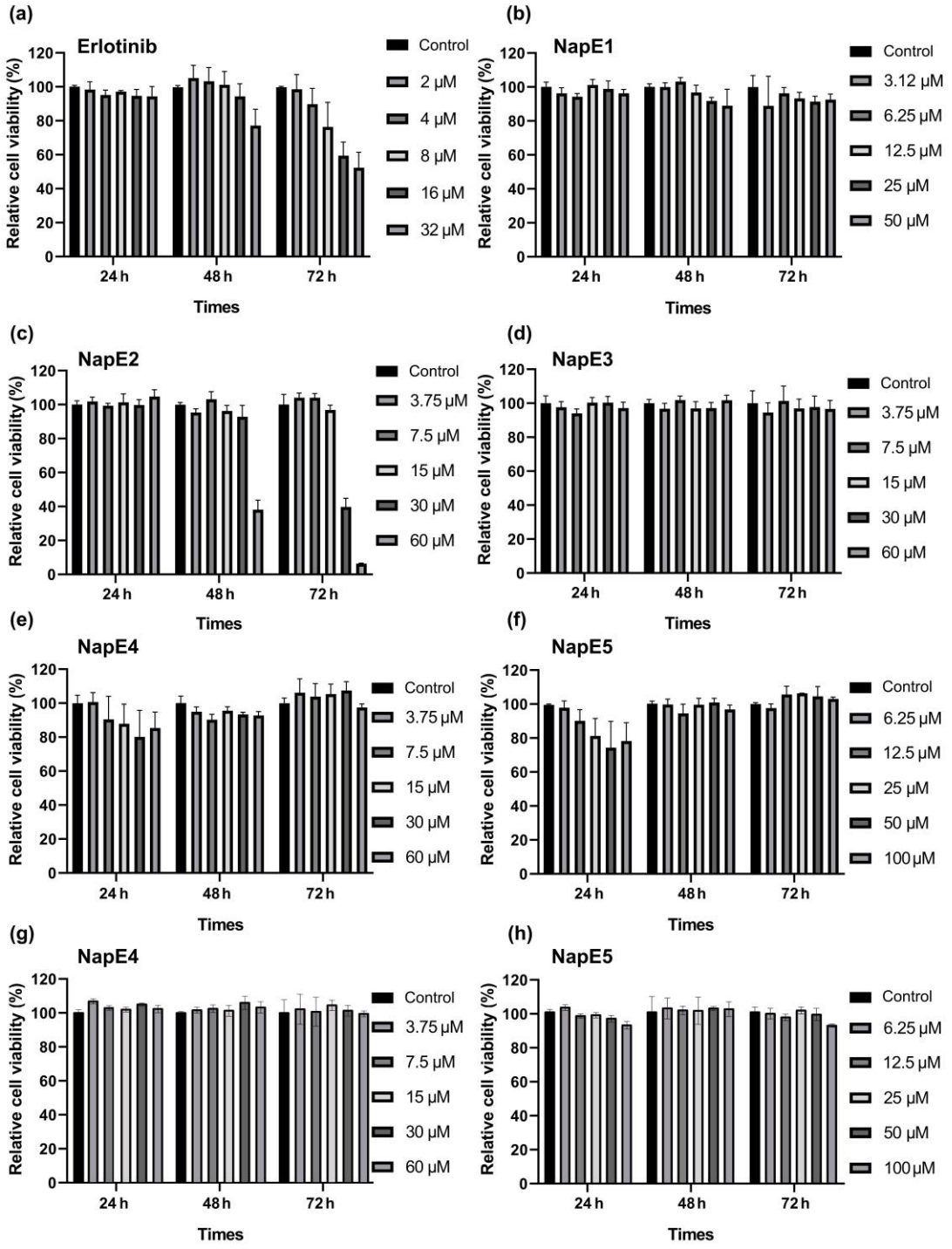

Figure S9. (a-f) Cell viability of A549 cells treated with different concentrations of Eriotinib and **NapE1-5** at different times; (g-h) Cell viability of BEAS-2B cells treated with different concentrations of **NapE4-5** at different times.

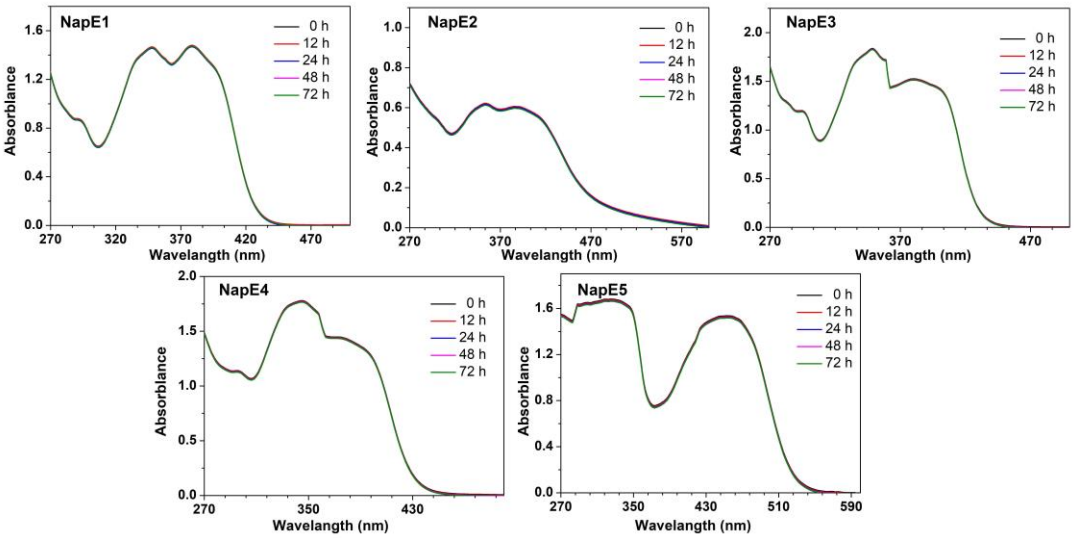

Figure S10. UV-vis absorption spectra of compounds (20 μM) in mixed solvents (PBS buffer solution : DMSO = 95 : 5) during incubation at different times.

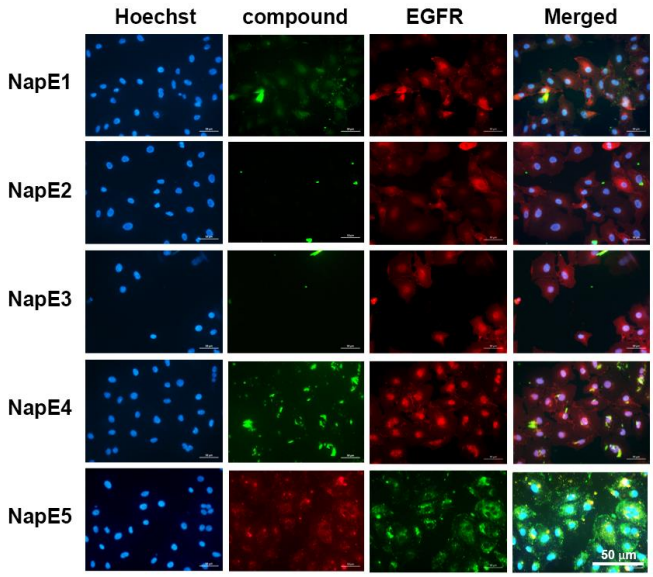

Figure S11. Confocal microscopy images of A549 cells incubated with **NapE1-5** compounds, Hoechst and EGFR (60 µM, 48 h) (**NapE1-4**, λ_{ex} = 488 nm and λ_{em} = 500 − 600 nm; **NapE5**: λ_{ex} = 559 nm and λ_{em} = 600 − 720 nm, red EGFR: λ_{ex} = 559 nm and λ_{em} = 600 − 700 nm, green EGFR: λ_{ex} = 488 nm and λ_{em} = 500 − 600 nm, cell nuclei: λ_{ex} = 405 nm and λ_{em} = 400 − 500 nm). Scale bar = 50 µm.

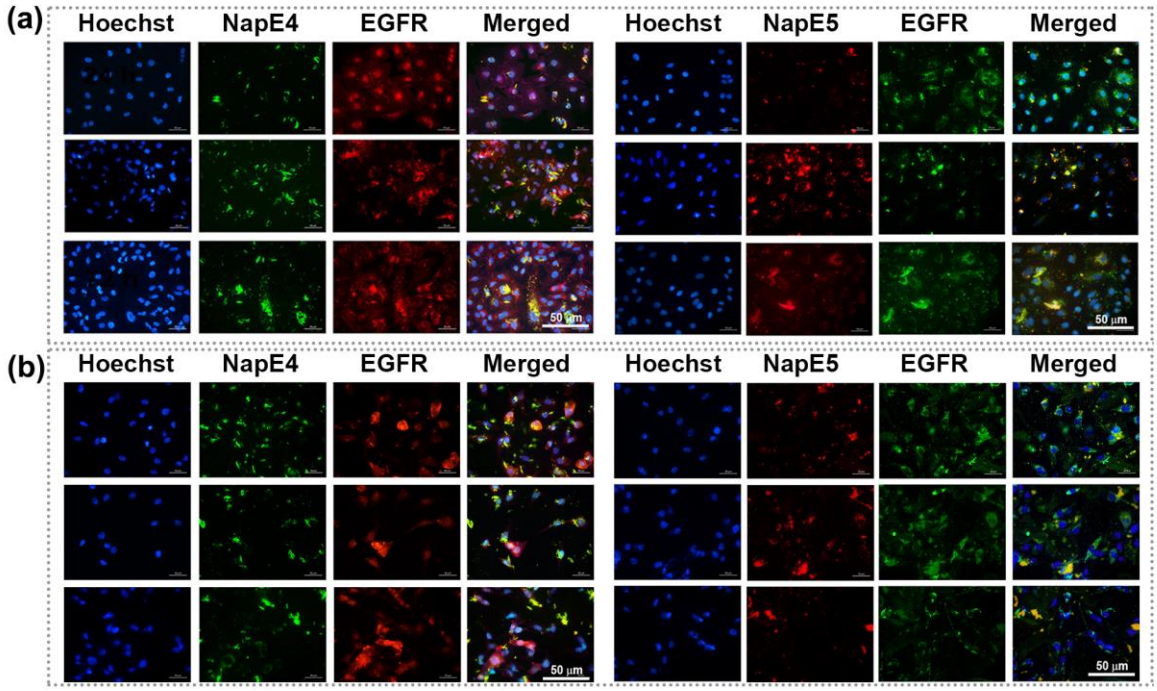

Figure S12. Confocal microscope images taken at 24, 48, and 72 hours of co-incubation of **NapE4** and **NapE5** with A549 cells (a) and H2228 cells (b) (**NapE4**: λ_{ex} = 488 nm and λ_{em} = 500 − 600 nm; EGFR: λ_{ex} = 559 nm and λ_{em} = 600 − 700 nm, cell nuclei: λ_{ex} = 405 nm and λ_{em} = 400 − 500 nm; **NapE5**: λ_{ex} = 559 nm and λ_{em}= 600 − 720 nm, EGFR: λ_{ex} = 488 nm and λ_{em} = 500 − 600 nm, Hoechst: λ_{ex} = 405 nm and λ_{em} = 400 − 500 nm). Scale bar = 50 µm.

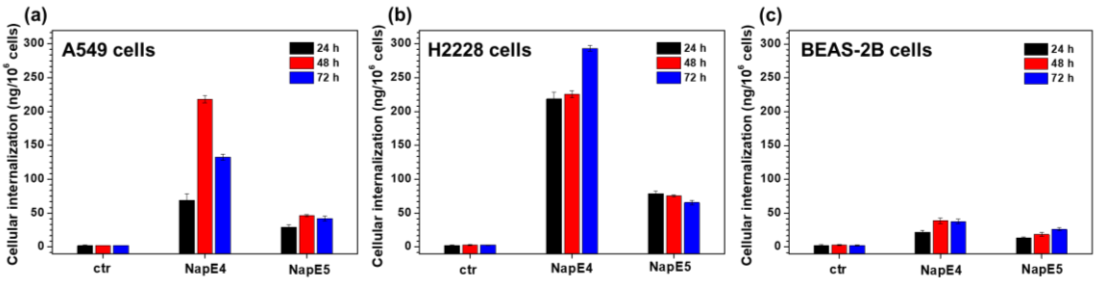

Figure S13. The boron contents of A549 (a), H2228 (b) and BEAS-2B (c) cells were incubated with **NapE4-5** (60 μM) (Control: the cells treated with no compound as the control group).

Table S4. The boron contents of compounds **NapE4-5** internalized by cancer cells and normal cells (Control: the cells treated with no compound as the control group).

Cancer cells	Compounds	B contents (ng/10^6cells)		
		24 h	**48 h**	**72 h**
A549 cells	**Control**	2.03 ± 1.00	2.40 ± 0.78	2.34 ± 1.24
	NapE4	68.85 ± 9.59	217.90 ± 5.08	132.54 ± 4.35
	NapE5	29.06 ± 4.03	46.28 ± 1.73	41.83 ± 3.44
H2228 cells	**Control**	2.13 ± 0.79	2.85 ± 0.54	2.74 ± 0.49
	NapE4	218.64 ± 9.59	225.76 ± 5.08	293.36 ± 4.35
	NapE5	78.41 ± 4.03	75.62 ± 1.73	65.44 ± 3.44
BEAS-2B cells	**Control**	2.57 ± 1.09	2.96 ± 1.07	2.36 ± 1.03
	NapE4	22.03 ± 2.63	38.75 ± 4.32	37.86 ± 3.40
	NapE5	13.52 ± 1.38	18.75 ± 3.35	26.11 ± 2.38

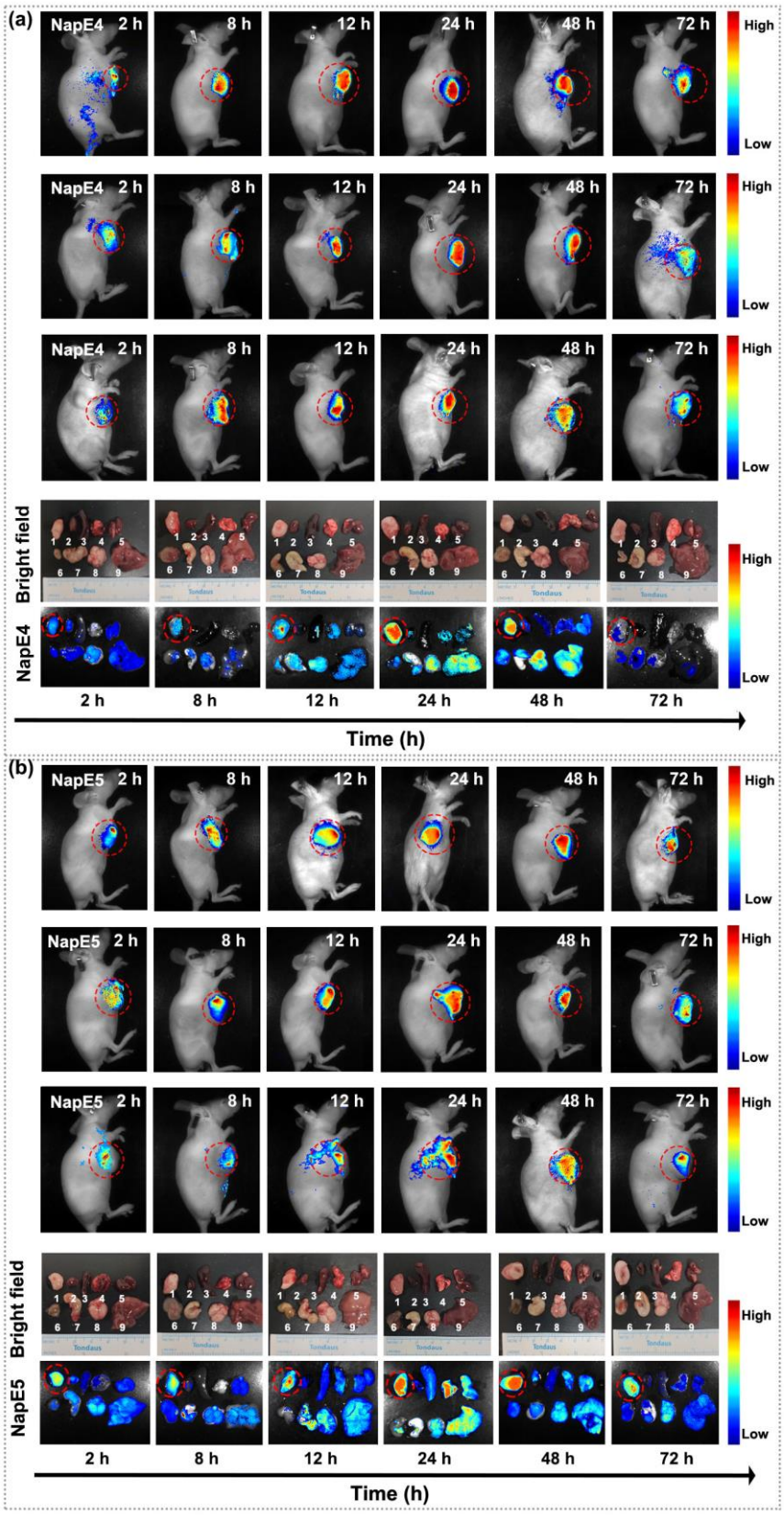

Figure S14. Fluorescence images of A549 tumor-bearing mice and selected organs at different times after intravenous injection of **NapE4** (a) and **NapE5** (b) (15 mg/kg).1: tumor; 2: heart; 3: spleen; 4: lung; 5: kidney; 6: intestine; 7:stomach; 8: brain; 9: liver (n = 6) (**NapE4**: λ_{ex} = 455 nm, λ_{em} = 500 − 670 nm, **NapE5**: λ_{ex} = 455 nm and λ_{em} = 580 − 750 nm). Here three sets of experimental data are presented.

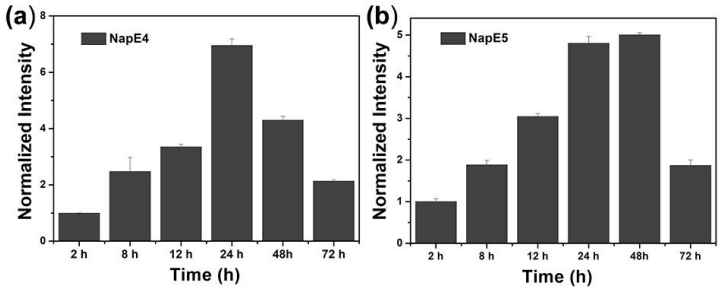

Figure S15. Normalized signal fluorescence intensities of **NapE4** (a) and **NapE5** (b) from the A549 tumor-bearing mice at different times after injection.

Table S5. The boron distribution of **NapE4** in A549 tumor-bearing mice at different times after injection (Data are expressed as mean ± SD, n = 6).

	Contents of boron (μg/g)					
	2 h	**8 h**	**12 h**	**24 h**	**48 h**	**72 h**
Tumor	6.52 ± 0.36	7.12 ± 0.42	7.77 ± 0.36	20.66 ± 1.23	15.72 ± 2.14	1.99 ± 0.01
Lung	0.92 ± 0.29	0.52 ± 0.23	0.66 ± 0.18	0.58 ± 0.23	0.51 ± 0.20	1.50 ± 0.13
Blood	0.75 ± 0.29	0.48 ± 0.04	0.33 ± 0.04	0.32 ± 0.04	0.33 ± 0.04	1.27 ± 0.01
Brain	1.08 ± 0.03	0.77 ± 0.16	0.65 ± 0.09	0.79 ± 0.06	0.67 ± 0.17	0.71 ± 0.02
Heart	1.33 ± 0.16	0.77 ± 0.07	0.72 ± 0.15	0.81 ± 0.10	0.78 ± 0.05	0.75 ± 0.06
Spleen	10.40 ± 0.48	1.05 ± 0.03	1.15 ± 0.13	1.00 ± 0.15	0.99 ± 0.06	0.90 ± 0.08
Kidney	3.05 ± 0.13	1.14 ± 0.03	1.00 ± 0.11	1.01 ± 0.22	1.35 ± 0.08	1.29 ± 0.19
Liver	16.52 ± 1.27	0.76 ± 0.06	0.72 ± 0.05	0.99 ± 0.06	0.89 ± 0.11	0.97 ± 0.12
Stomach	2.52 ± 0.10	2.10 ± 0.16	2.79 ± 0.16	1.67 ± 0.21	3.13 ± 0.29	3.41 ± 0.59
Intestine	2.74 ± 0.25	1.25 ± 0.05	1.06 ± 0.02	0.97 ± 0.03	0.90 ± 0.04	0.96 ± 0.14

Table S6. The tumor to normal tissue ratios (T/N) (**NapE4**) of boron contents of tissues from mice bearing A549 tumor at different times.

	T/N ratios					
	2 h	**8 h**	**12 h**	**24 h**	**48 h**	**72 h**
Tumor /Lung	7.08 ± 0.32	13.57 ± 0.33	11.70 ± 0.27	35.70 ± 0.73	30.61 ± 1.17	1.33 ± 0.07
Tumor /Blood	8.71 ± 0.55	14.71 ± 0.45	23.84 ± 0.34	64.03 ± 0.78	47.33 ± 1.24	1.57 ± 0.64
Tumor /Heart	4.91 ± 0.26	9.21 ± 0.24	10.86 ± 0.26	25.55 ± 0.66	20.20 ± 1.10	2.65 ± 0.04
Tumor /Spleen	0.63 ± 0.42	6.80 ± 0.23	6.76 ± 0.24	20.64 ± 0.69	15.85 ± 1.10	2.21 ± 0.05
Tumor /Brain	6.02 ± 0.20	9.30 ± 0.29	11.98 ± 0.22	26.25 ± 0.64	23.33 ± 1.15	2.81 ± 0.01
Tumor /Kidney	2.14 ± 0.25	6.22 ± 0.23	7.73 ± 0.23	20.48 ± 0.72	11.68 ± 1.11	1.55 ± 0.10
Tumor /Liver	0.39 ± 0.81	9.42 ± 0.24	10.79 ± 0.20	20.85 ± 0.64	17.72 ± 1.13	2.06 ± 0.07
Tumor /Stomach	2.59 ± 0.23	3.39 ± 0.29	2.79 ± 0.26	12.40 ± 0.72	5.02 ± 1.21	0.58 ± 0.30
Tumor /Intestine	2.38 ± 0.30	5.71 ± 0.23	7.32 ± 0.19	21.38 ± 0.63	17.41 ± 1.09	2.07 ± 0.08

Table S7. The boron distribution of **NapE5** in A549 tumor-bearing mice at different times after injection (Data are expressed as mean ± SD, n = 6).

	Contents of boron (μg/g)					
	2 h	**8 h**	**12 h**	**24 h**	**48 h**	**72 h**
Tumor	5.57 ± 0.35	7.33 ± 0.27	9.30 ± 0.28	23.41 ± 1.02	24.67 ± 1.19	6.11 ± 0.18
Lung	1.27 ± 0.47	0.64 ± 0.16	0.68 ± 0.21	0.41 ± 0.24	3.63 ± 0.28	2.50 ± 0.02
Blood	0.84 ± 0.01	0.63 ± 0.02	0.67 ± 0.03	0.27 ± 0.04	0.66 ± 0.03	1.39 ± 0.09
Brain	1.21 ± 0.05	0.73 ± 0.06	0.67 ± 0.25	0.70 ± 0.08	0.94 ± 0.18	0.84 ± 0.07
Heart	0.86 ± 0.04	0.87 ± 0.04	0.97 ± 0.10	0.81 ± 0.10	1.03 ± 0.13	0.69 ± 0.09
Spleen	2.04 ± 0.15	1.18 ± 0.06	0.87 ± 0.37	0.85 ± 0.05	1.04 ± 0.29	0.90 ± 0.10
Kidney	1.96 ± 0.02	1.66 ± 0.15	1.78 ± 0.28	0.86 ± 0.10	0.95 ± 0.09	3.89 ± 0.22
Liver	2.09 ± 0.12	1.21 ± 0.05	0.76 ± 0.21	0.77 ± 0.17	1.34 ± 0.24	1.27 ± 0.05
Stomach	10.97 ± 0.90	3.77 ± 0.33	1.88 ± 0.17	1.65 ± 0.16	3.74 ± 0.16	2.52 ± 0.07
Intestine	1.90 ± 0.11	1.08 ± 0.14	1.07 ± 0.06	0.77 ± 0.07	0.95 ± 0.08	1.07 ± 0.14

Table S8. The tumor to normal tissue ratios (T/N) (**NapE5**) of boron contents of tissues from mice bearing A549 tumor at different times.

	T/N ratios					
	2 h	**8 h**	**12 h**	**24 h**	**48 h**	**72 h**
Tumor /Lung	4.38 ± 0.41	11.40 ± 0.21	13.71 ± 0.24	57.70 ± 0.63	6.80 ± 0.74	2.45 ± 0.10
Tumor /Blood	6.61 ± 0.60	11.70 ± 0.45	13.80 ± 0.48	86.17 ± 0.65	37.62 ± 0.93	4.41 ± 0.78
Tumor /Heart	6.49 ± 0.20	8.42 ± 0.15	9.55 ± 0.19	28.94±0.56	23.92 ± 0.66	8.84 ± 0.13
Tumor /Spleen	2.74 ± 0.25	6.24 ± 0.16	0.91 ± 0.46	27.42 ± 0.54	1.72 ± 1.16	6.77 ± 0.14
Tumor /Brain	4.61 ± 0.20	10.04 ± 0.16	13.91 ± 0.26	33.43 ± 0.55	26.30 ± 0.69	7.24 ± 0.12
Tumor /Kidney	2.84 ± 0.19	4.43 ± 0.21	5.24 ± 0.28	27.09 ± 0.56	25.90 ± 0.64	1.57 ± 0.20
Tumor /Liver	2.67 ± 0.24	6.03 ± 0.16	0.37 ± 1.23	30.45 ± 0.60	1.43 ± 1.06	4.83 ± 0.11
Tumor /Stomach	0.51 ± 0.63	1.95 ± 0.30	4.95 ± 0.22	14.21 ± 0.59	6.60 ± 0.68	2.43 ± 0.12
Tumor /Intestine	2.93 ± 0.23	6.80 ± 0.20	8.70 ± 0.17	30.36 ± 0.55	25.88 ± 0.64	5.69 ± 0.16

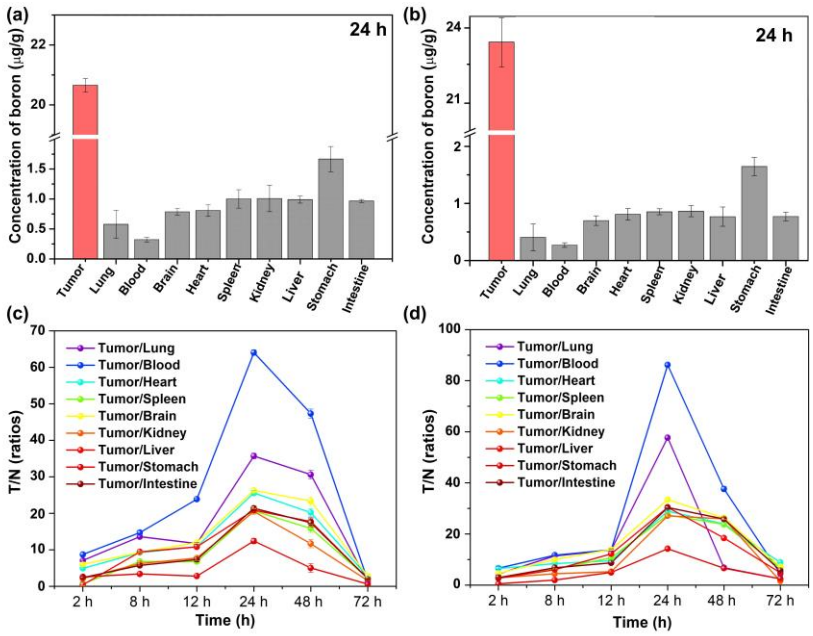

Figure S16. The boron content distribution detected in mice injected with **NapE4** (a) and **NapE5** (b) after 24 hours (n = 6). The T/N ratios (**NapE4** (c) and **NapE5** (d)) of the boron contents from mice bearing A549 tumor at different times at room temperature.

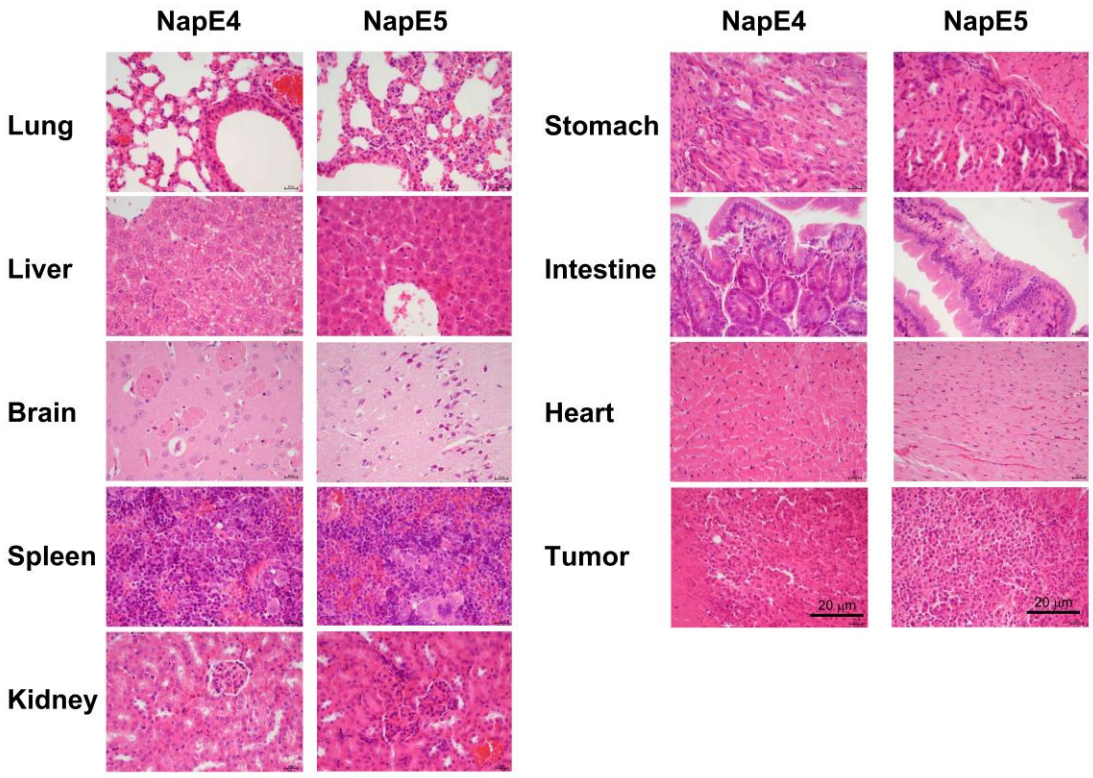

Figure S17. H&E staining images of major organs of mice administrated by single intravenous injection with compounds **NapE4-5** for one week (n = 3).

Table S9. The boron contents of **^{10}B-NapE4** internalized by cancer cells at 48 h (Control: the cells treated with no compound applied).

Cancer cells	Concentration	^{10}B (ng/10^{6}cells)
A549 cells	Control	4.94 ± 1.10
	30 μM	57.28 ± 4.40
	45 μM	133.62 ± 0.60
	60 μM	176.82 ± 5.30

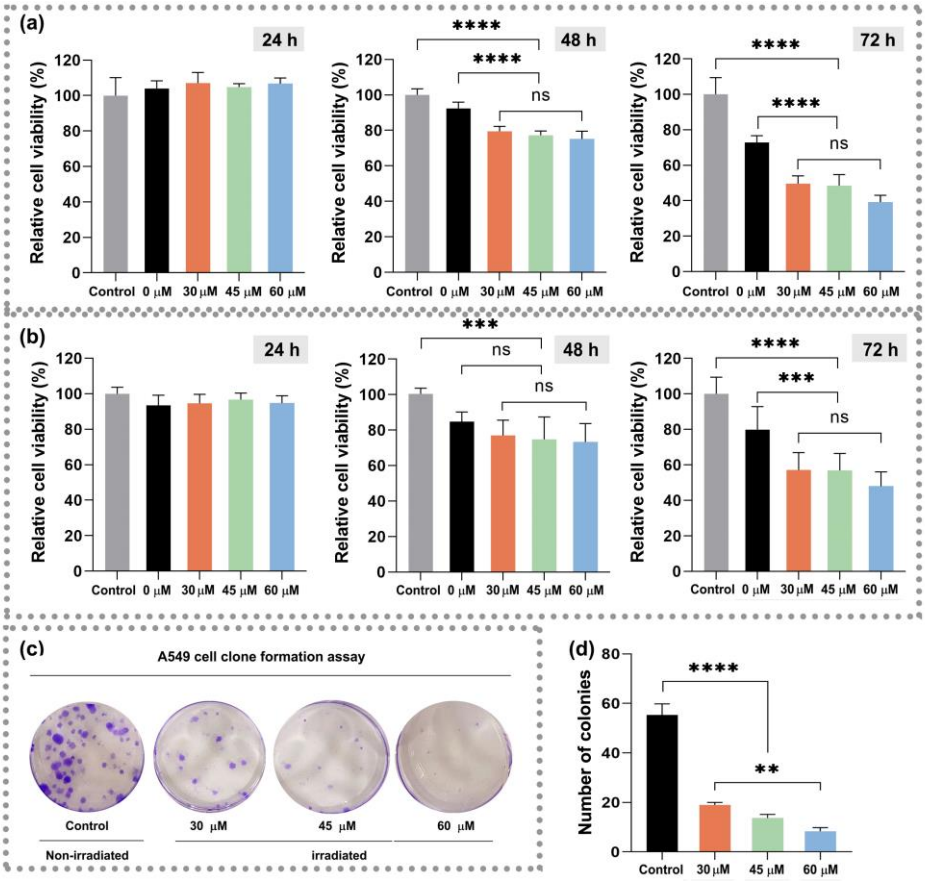

Figure S18. A549 cancer cells treated with different concentrations of **^{10}B-NapE4**, then subjected to neutron irradiation for 26 min (high dose) (a) and for 17 min (low dose) (b), the comparison of the A549 cell viability at different times after irradiation (The control group was not exposed to neutron irradiation with no boron applied). (c) The clone formation assay of irradiated A549 cells observed on the 14th day. (d) Quantitative data of colonies on the 14th day after neutron irradiation. P values = ****p < 0.0001; ***p < 0.001. ns: no significance. The control group unexposed to neutron irradiation with no boron carrier applied.

Table S10. Cell viability of A549 treated with different concentrations of **^{10}B-NapE4** at different times after neutron irradiation (high dose: 26 min, low dose: 17 min, epithermal neutron flux: 8.015×10^8 n cm^{-2} s^{-1}).

Relative cell viability (%)				
		24 h	**48 h**	**72 h**
Low dose	0 μM	93.46 ± 2.53	84.46 ± 2.39	79.84 ± 5.30
	30 μM	94.51 ± 2.05	76.65 ± 3.86	57.15 ± 3.99
	45 μM	96.63 ± 1.65	74.43 ± 5.64	56.82 ± 3.91
	60 μM	94.65 ± 1.88	72.90 ± 4.67	47.97 ± 3.28
High dose	0 μM	103.90 ± 2.18	92.38 ± 1.61	72.89 ± 1.88
	30 μM	107.10 ± 2.98	79.45 ± 1.27	49.54 ± 2.67
	45 μM	104.80 ± 0.98	77.19 ± 1.11	48.43 ± 3.17
	60 μM	106.80±1.57	75.10±1.98	39.11 ± 1.97

Table S11. Quantitative data of colonies on the 14th day after irradiation (the control group unexposed to neutron irradiation with no boron carrier applied).

Cells clone formation assay (high dose)			
Control	30 μM	45 μM	60 μM
55.33±4.51	19.00 ± 1.00	13.67 ± 1.53	8.33 ± 1.53

Table S12. The boron contents and T/N ratios of **^{10}B-NapE4** internalized by each organ of A549 tumor-bearing mice at 24 h at room temperature (Data are expressed as mean ± SD, n = 3).

Contents of boron (μg/g)				T/N ratios			
Tumor	22.66 ± 3.28	**Liver**	0.50 ± 0.36	**Tumor/ Lung**	35.42 ± 1.84	**Tumor/ Brain**	48.41 ± 2.10
Lung	0.64 ± 0.40	**Brain**	0.47 ± 0.30	**Tumor/ Blood**	28.93 ± 2.29	**Tumor/ Intestine**	52.60 ± 1.70
Blood	0.84 ± 0.01	**Intestine**	0.49 ± 0.27	**Tumor/ Stomach**	26.98 ± 2.31	**Tumor/Spleen**	24.54 ± 1.19
Stomach	0.78 ± 0.04	**Spleen**	0.92 ± 0.29	**Tumor/ Heart**	33.51 ± 1.91	**Tumor/Kidney**	31.95 ± 1.86
Heart	0.68 ± 0.57	**Kidney**	0.70 ± 0.65	**Tumor/ Liver**	45.42 ± 2.06		

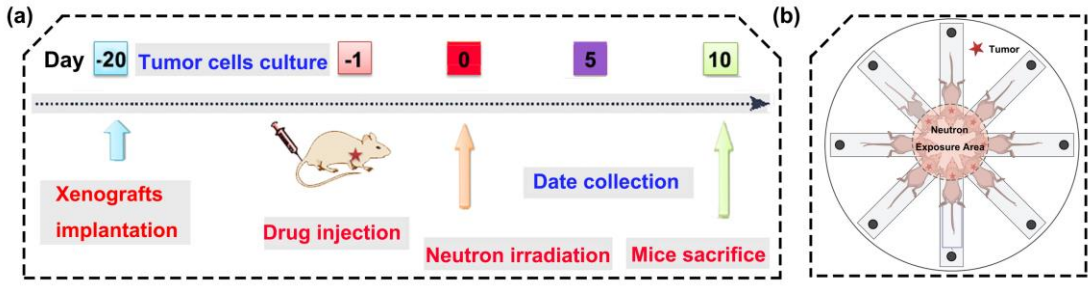

Figure S19. (a) Scheme of experimental timeline for neutron irradiation experiments. (b) Illustration of the mouse fixation apparatus. The mouse tumor was fixed within the neutron exposure area (Created with MedPeer (www.medpeer.cn)).

Table S13. Exposure time of each group of mice to neutron beams on the NeuPex^{TM} Block-I AB-BNCT system (Epithermal neutron flux: 8.015 × 10^8 n cm^{-2} s^{-1}): L BNCT: **^{10}B-NapE4** + neutron irradiation of 7 minutes = radioactive dose of 1.0 Gy; M BNCT: **^{10}B-NapE4** + neutron irradiation of 10 minutes = radioactive dose of 1.5 Gy; H BNCT: **^{10}B-NapE4** + neutron irradiation of 14 minutes = radioactive dose of 2.0 Gy. Statistical analysis was performed using Monte Carlo.

		Exposure duration (min)
Mice experiments	**L BNCT**	7 (= 1.0 Gy dose)
	M BNCT	10 (= 1.5 Gy dose)
	H BNCT	14 (= 2.0 Gy dose)

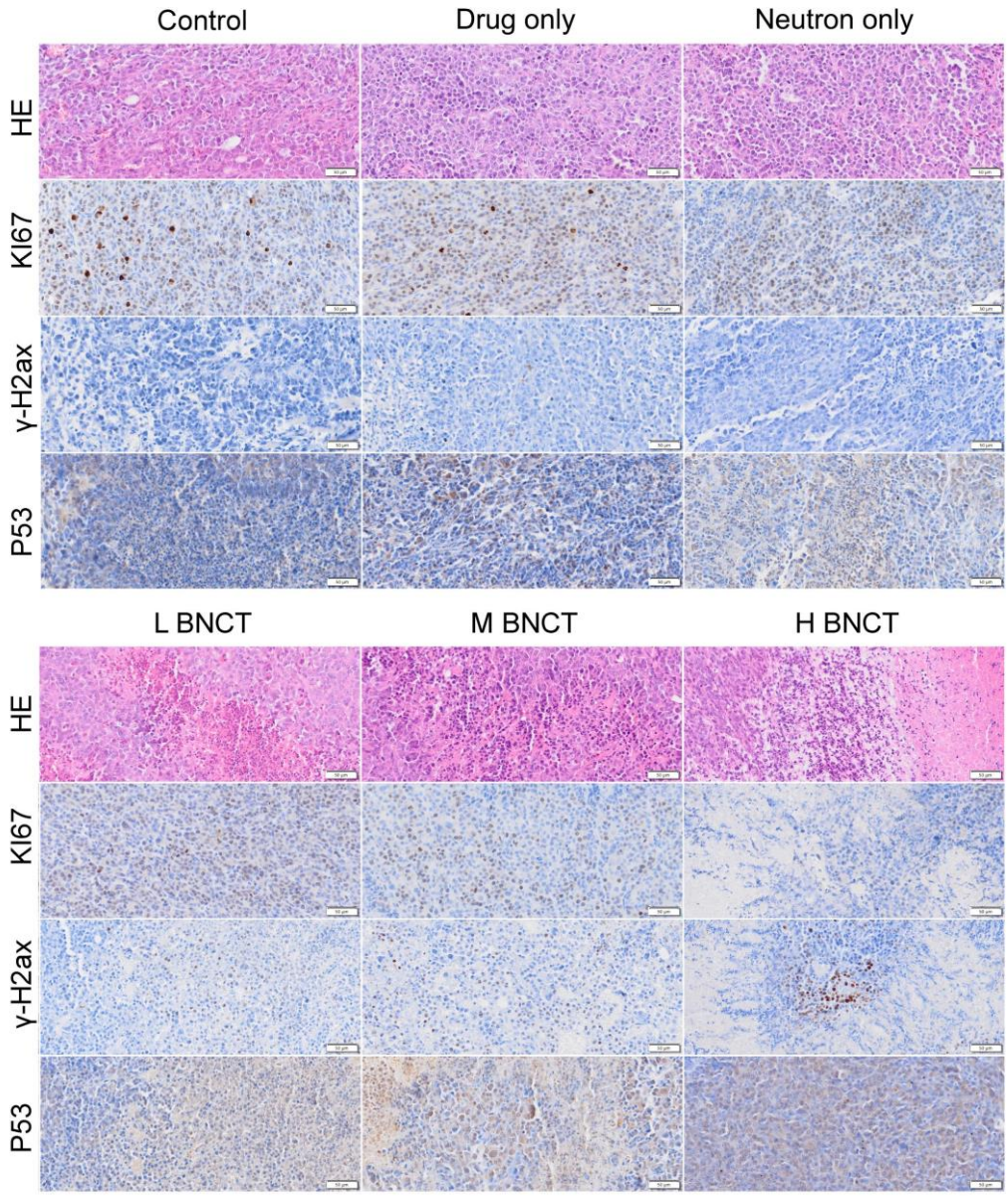

Figure S20. Pathological and immunohistochemical results. Representative pathological images of apoptosis and proliferation in tumor tissues.

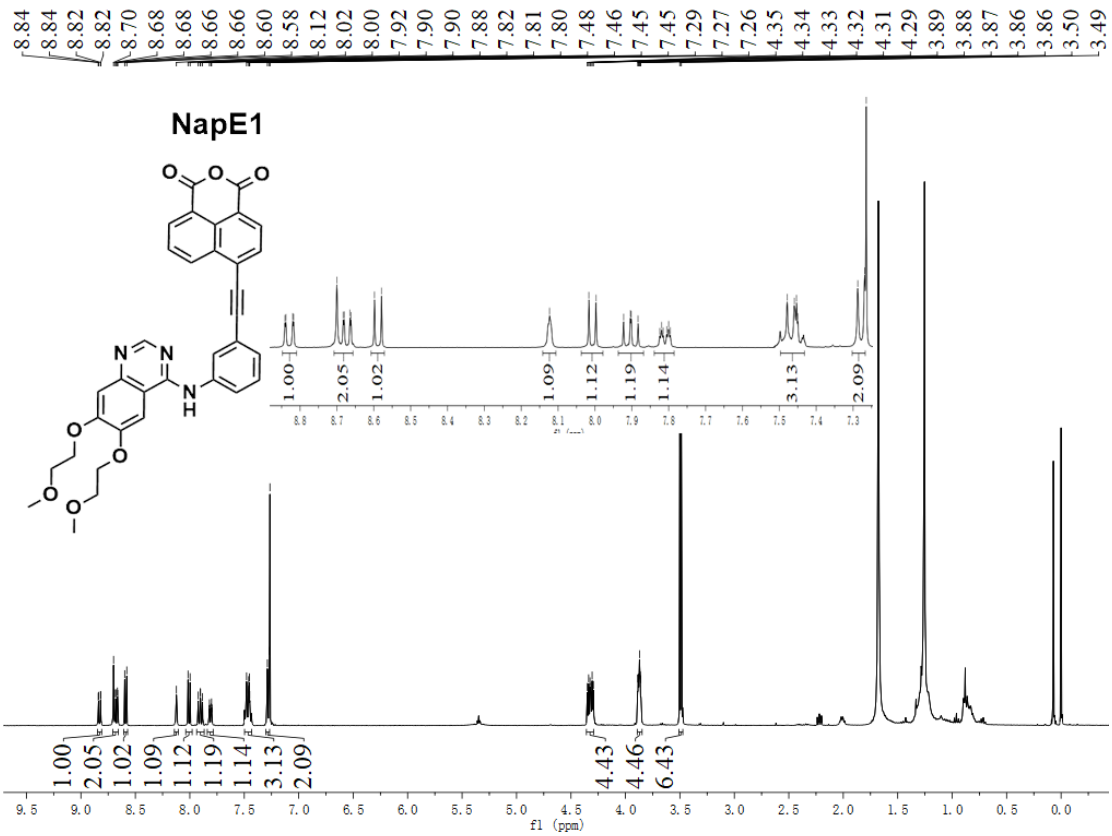

Figure S21. ^{1}H NMR (400 MHz, $CDCl_3$).

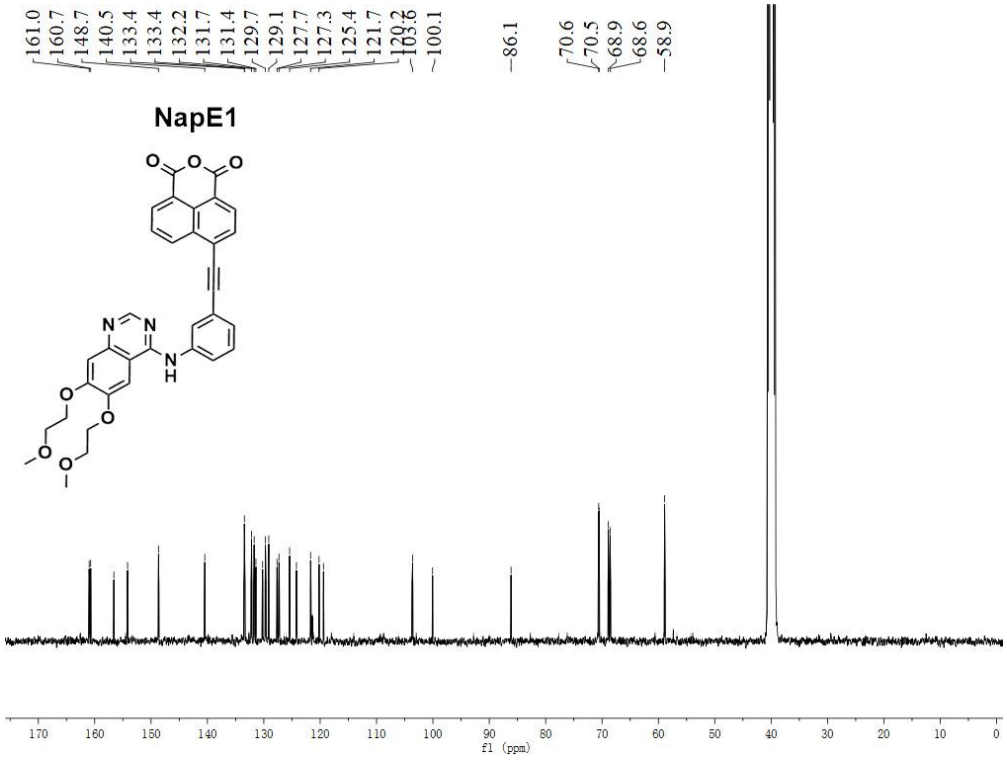

Figure S22. ^{13}C NMR (400 MHz, DMSO-d_6).

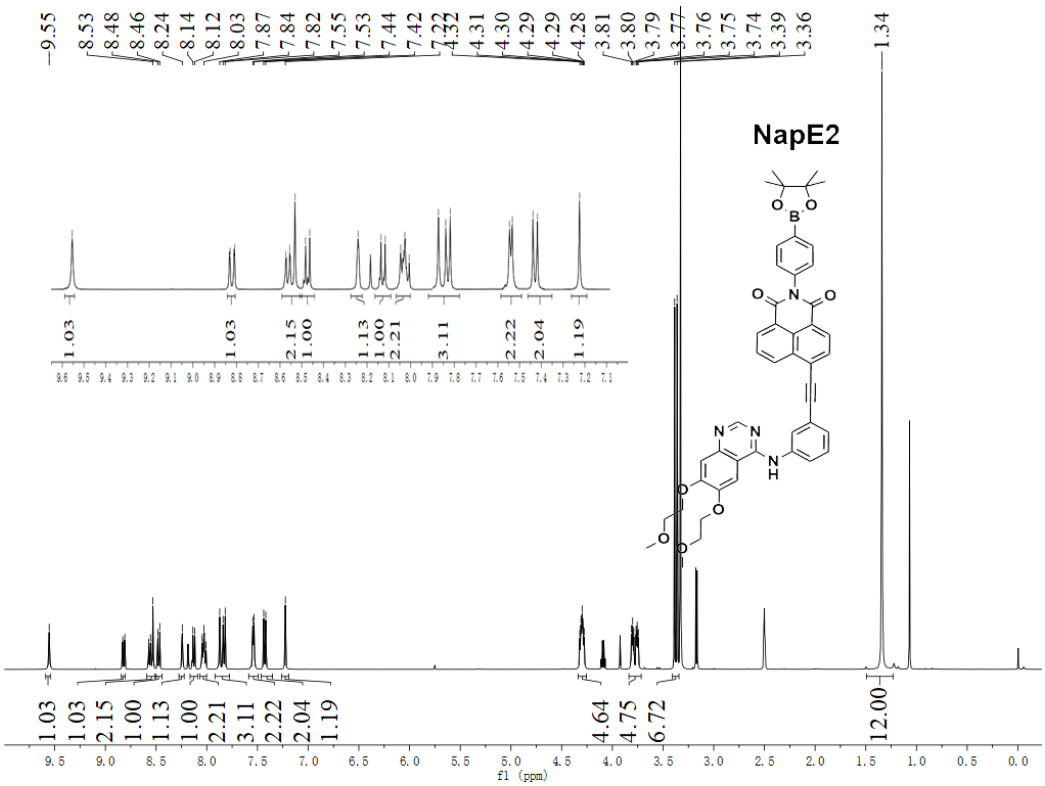

Figure S23. ^{1}H NMR (400 MHz, DMSO-d_6).

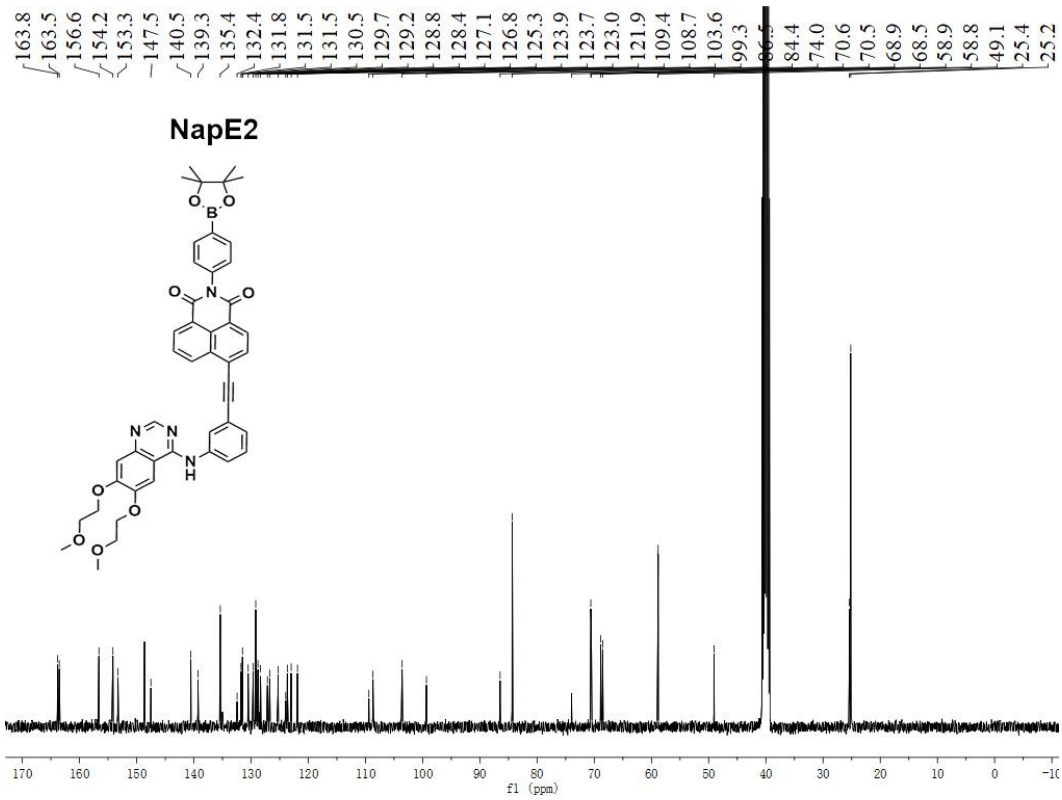

Figure S24. ^{13}C NMR (126 MHz, DMSO-d_6).

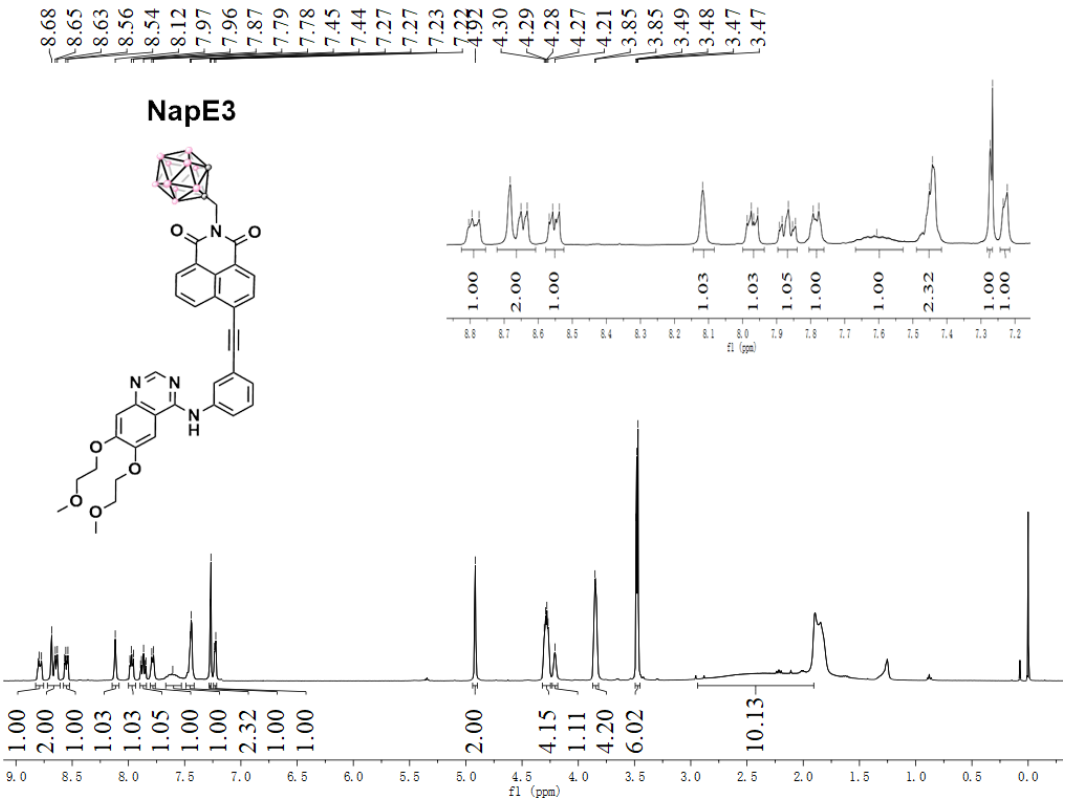

Figure S25. ^{1}H NMR (400 MHz, $CDCl_3$).

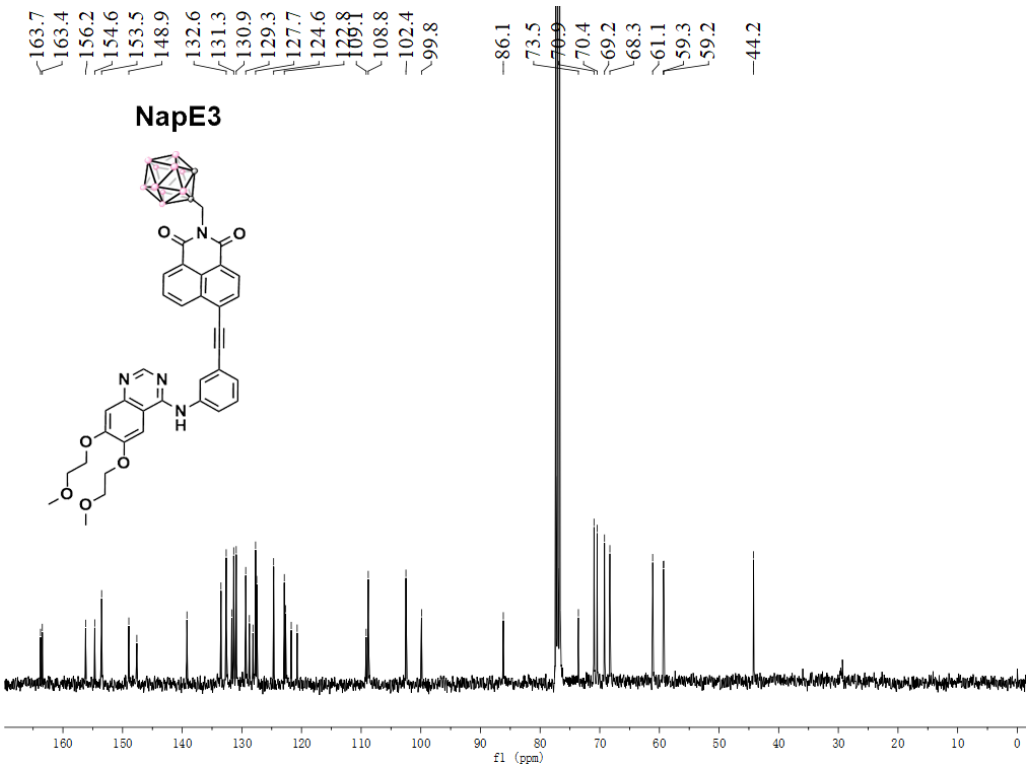

Figure S26. ^{13}C NMR (126 MHz, $CDCl_3$).

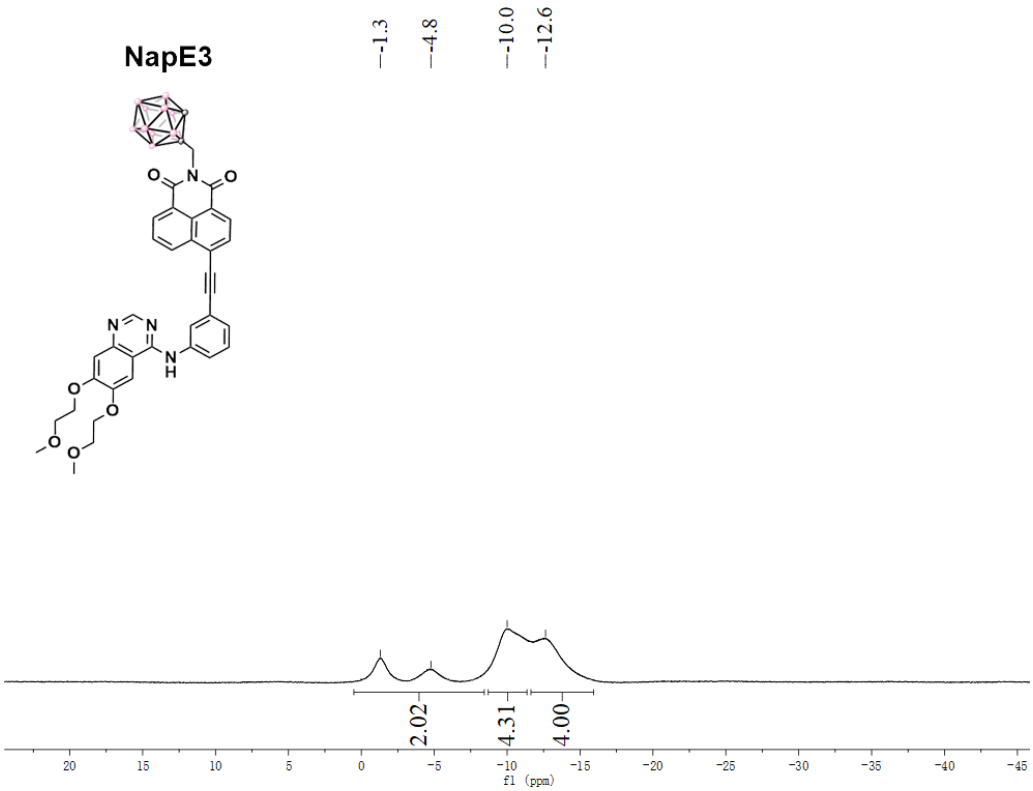

Figure S27. $^{11}B\{^{1}H\}$ NMR (128 MHz, $CDCl_3$).

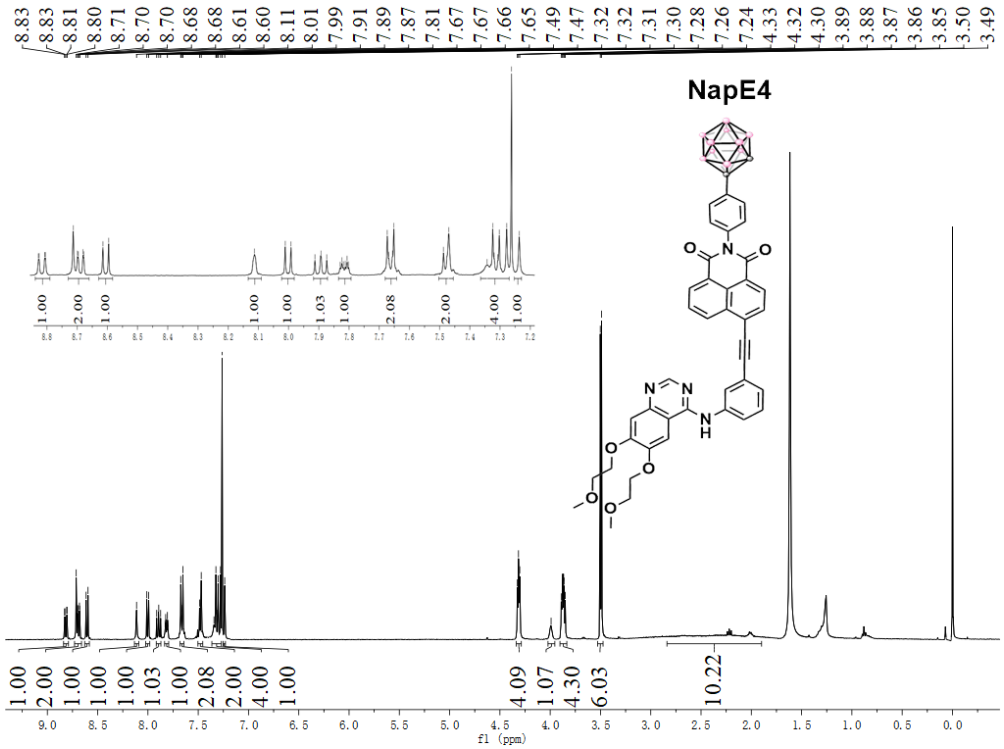

Figure S28. ^{1}H NMR (400 MHz, $CDCl_3$).

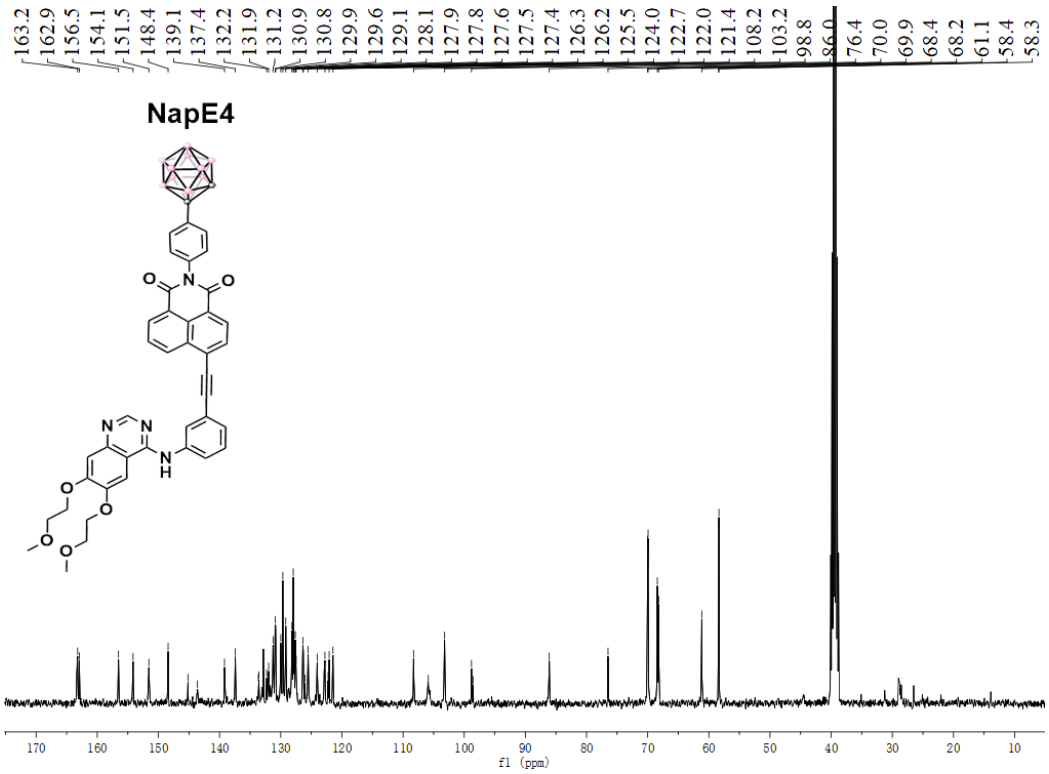

Figure S29. ^{13}C NMR (126 MHz, DMSO-d_6).

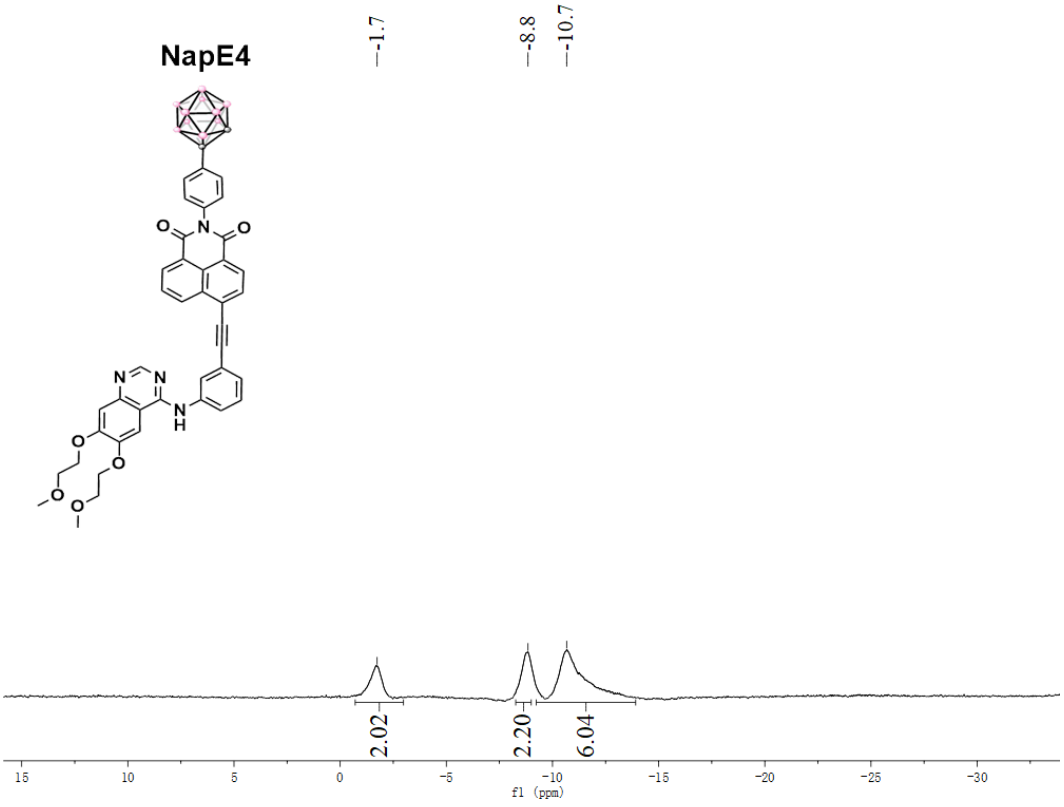

Figure S30. $^{11}B\{^{1}H\}$ NMR (128 MHz, $CDCl_3$).

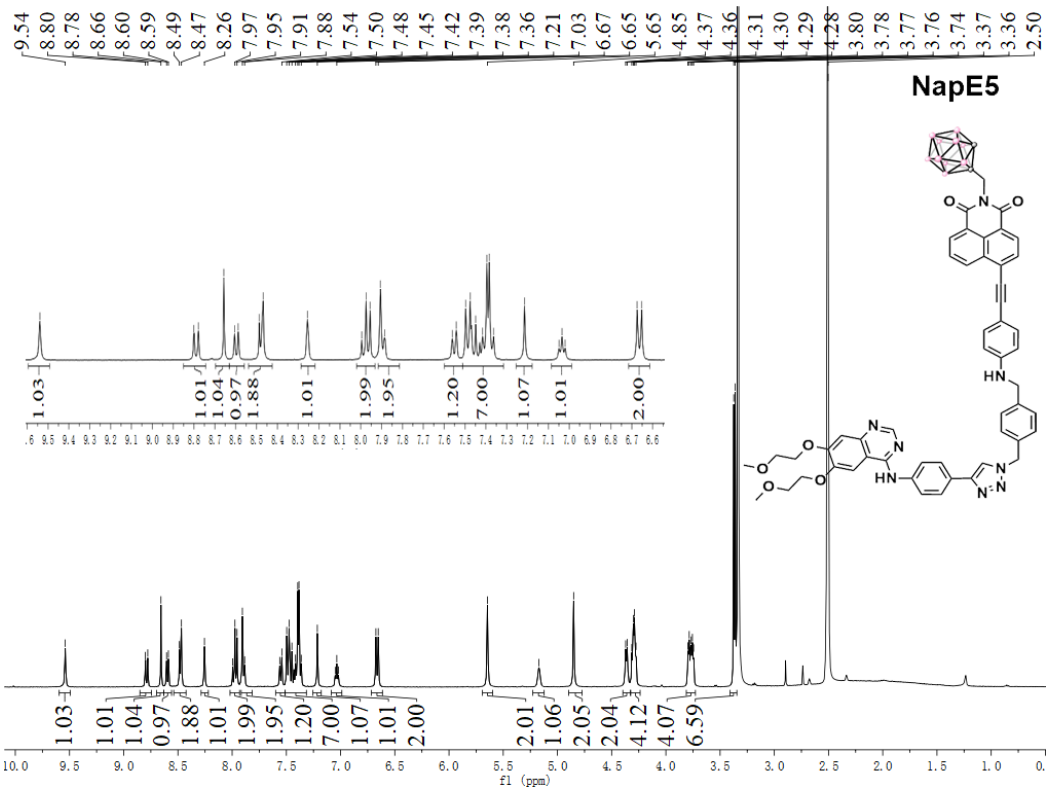

Figure S31. ^{1}H NMR (400 MHz, DMSO-d_6).

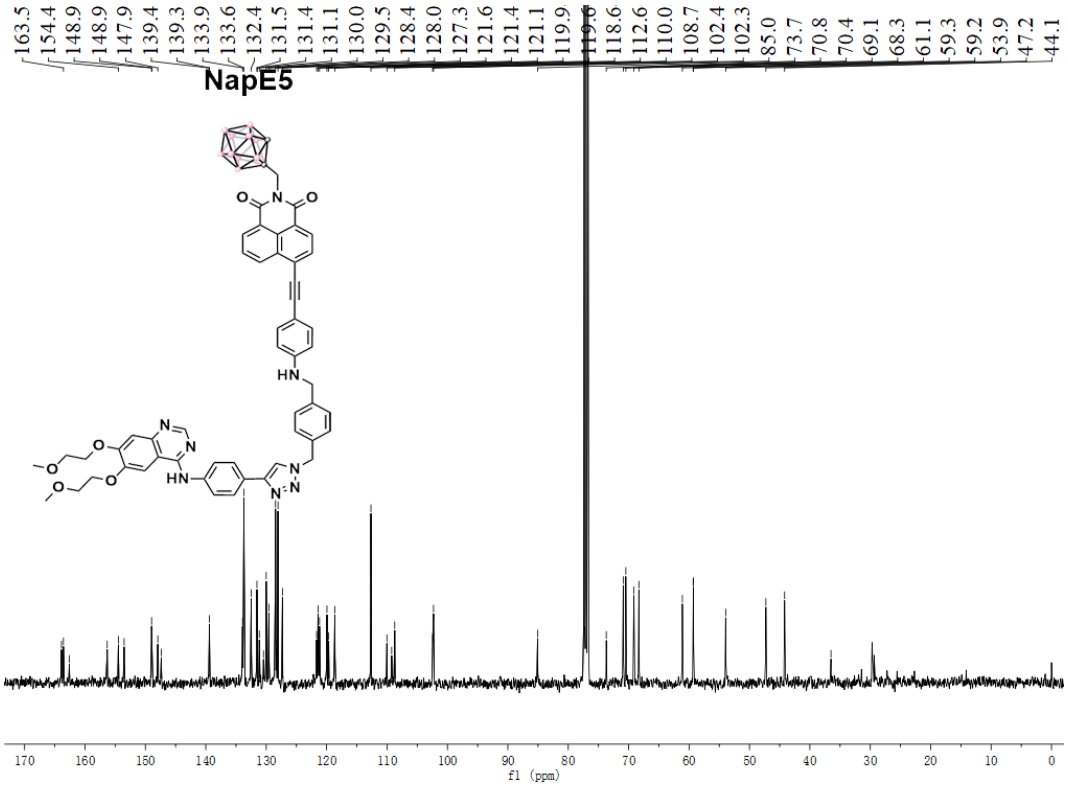

Figure S32. ^{13}C NMR (126 MHz, $CDCl_3$).

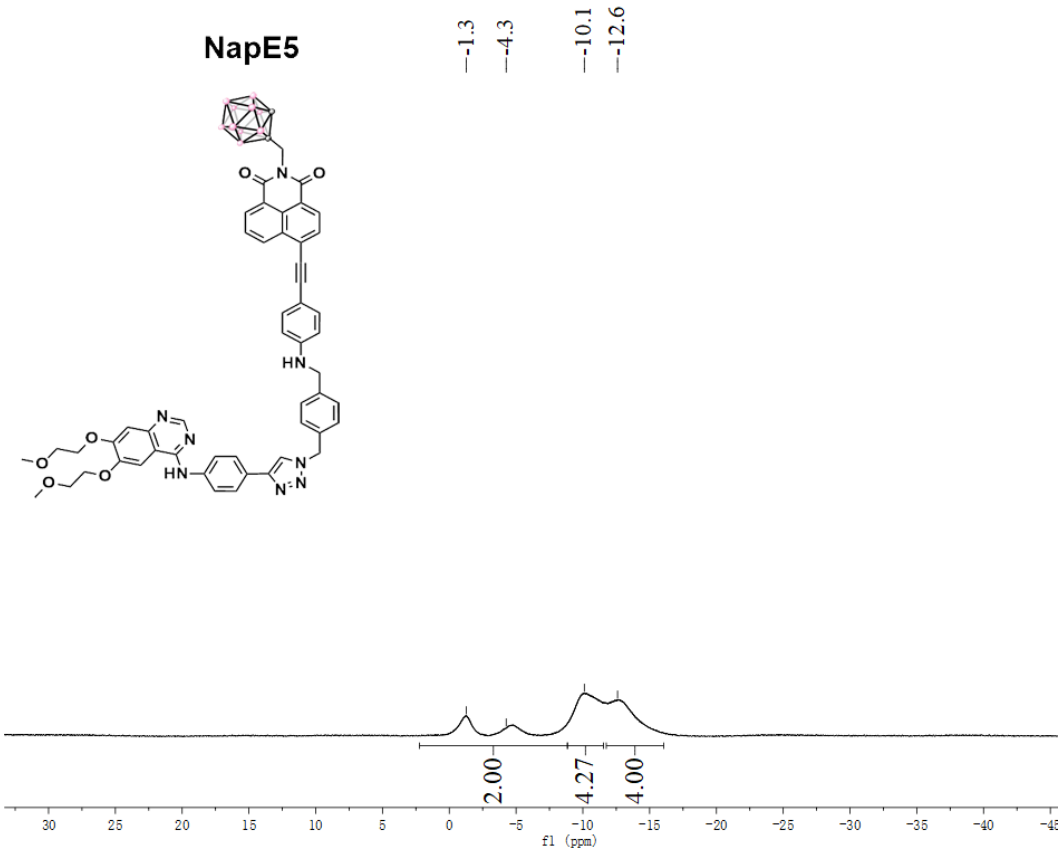

Figure S33. $^{11}B\{^{1}H\}$ NMR (128 MHz, DMSO-d_6).

Reference

1 Frisch, M. J. et al. Gaussian 16, Rev. A. 03; Gaussian Inc.: *Wallingford*, CT, 2016.

2 Park, R.; Chang, C.-C.; Liang, Y.-C.; Chung, Y.; Henry, R. A.; Lin, E.; Mold, D.; Huang, R. C. C. *Clin. Cancer Res.* 2005, **11**, 4601−4609.

3 L.Fang, G. Trigiante, C. Kousseff, R. Crespo-Otero, M. Philpottb, M. Watkinson, *Chem. Commun.* 2018, **54**, 9619.

4 T. Zhao, V. Lynch, J. Sessler, *Org. Biomol. Chem.* 2022, **20**, 980.